NASA Technical Memorandum 104317

A Historical Perspective of the YF-12A Thermal Loads and Structures Program

Jerald M. Jenkins and Robert D. Quinn

May 1996

National Aeronautics and
Space Administration

NASA Technical Memorandum 104317

A Historical Perspective of the YF-12A Thermal Loads and Structures Program

Jerald M. Jenkins and Robert D. Quinn
NASA Dryden Flight Research Center
Edwards, California

1996

National Aeronautics and
Space Administration

Dryden Flight Research Center
Edwards, California 93523-0273

ABSTRACT

Around 1970, the YF-12A loads and structures efforts focused on numerous technological issues that needed defining with regard to aircraft that incorporate hot structures in the design. Laboratory structural heating test technology with infrared systems was largely created during this program. The program demonstrated the ability to duplicate the complex flight temperatures of an advanced supersonic airplane in a ground-based laboratory. The ability to heat and load an advanced operational aircraft in a laboratory at high temperatures and return it to flight status without adverse effects was demonstrated. The technology associated with measuring loads with strain gages on a hot structure was demonstrated with a thermal calibration concept. The results demonstrated that the thermal stresses were significant although the airplane was designed to reduce thermal stresses. Considerable modeling detail was required to predict the heat transfer and the corresponding structural characteristics. The overall YF-12A research effort was particularly productive, and a great deal of flight, laboratory, test and computational data were produced and cross-correlated.

INTRODUCTION

More than 20 yr have passed since completion of YF-12A Thermal Loads and Structures Program. This program was one of the most comprehensive flight and laboratory hot structures and loads research efforts ever undertaken (ref. 1). The primary tools used to accomplish this program were the triple sonic YF-12A aircraft and the NASA Dryden Flight Research Center (DFRC), Thermostructures Research Facility, Edwards, California. This facility is a major ground-based aeronautical high-temperature research laboratory. Computational efforts associated with the flight and laboratory also enhanced these activities. Few high-speed vehicles have evolved in the past 25 yr; therefore, the science of dealing with major aerodynamically heated flight structures has been minimally developed. The basic technical approaches to conducting the program, coupled with the technical results, are still a model worthy of historical documentation. An unusually long period of classification, the large amount of elapsed time since the effort was completed, and the diminishing number of people associated with the program who are still professionally active is posing the threat of losing the importance and the details of the effort.

This paper describes the salient technical results of the YF-12A structures and loads efforts, so the experiences and results can be preserved. Use of trade names or names of manufacturers in this report does not constitute an official endorsement of such products or manufacturers, either expressed or implied, by NASA.

BASIC TECHNICAL ISSUES AND ASSOCIATED HISTORY

Aeronautical interests of the 1950's and 1960's greatly emphasized high-speed aircraft. Such interests resulted in aircraft, such as the X-15 and XB-70 (North American Aviation, Downey, California), F-111 (General Dynamics, Fort Worth, Texas), and YF-12A and SR-71 (Lockheed Corporation, Burbank, California) aircraft (refs. 1–6), which were all directed toward speeds of Mach 2.7 or greater. Before development of these aircraft, there was an evolving science directed toward measuring flight loads on airplanes using calibrated strain gages. The advent of aircraft with Mach 2.7 plus capabilities introduced a problem that complicated the measurement of loads with strain gages. Aerodynamic heating of the structure was so intense that significant structural temperature nonuniformities resulted in major thermal stress fields within the structures of these high-speed aircraft. These thermal stress fields resulted in an

additional component of strain that affected the strain gage calibration used to measure the flight loads. Strain gages used on these high-speed aircraft sensed responses to the aerodynamic loads and thermal stresses. This response created a major problem in the 1960's because verifying the design of a new military aircraft required conducting a flight loads survey and structural integrity flight demonstration using calibrated strain gages as the verifying tool. This approach was dictated by military specifications for new aircraft.

The major problem with measuring strain gage loads on hot structures was first addressed on the X-15 aircraft. Strain gage flight loads were never measured on the X-15 because of the extreme temperatures and the thermal stress fields (refs. 7 and 8). The X-15 Program resulted in a recognition that a need existed to understand the effects of temperature on strain gages and structures. This lack of understanding led to the construction of a major ground-based laboratory capable of heating an entire aircraft (ref. 9) at NASA DFRC in the late 1960's. The facility was built to help understand high-temperature effects on hot aircraft. The laboratory was originally called the Flight Loads Research Facility and is presently called the Thermostructures Research Facility.

Computational software, such as NASA Structural Analysis (NASTRAN), was available in the 1960's which could provide thermal stress computing capabilities; however, computers had little capacity to conduct large computations. Because little could be done about this problem computationally, it was decided to attack the problem experimentally. The basic approach involved heating the structure on the ground in a laboratory to the exact temperature environment that the structure witnessed in flight. This temperature environment would impose a thermal stress field on the structure identical to that which occurred in flight. The responses of the strain gages measured in the laboratory would serve as a correction for the flight data. Hence, the thermal response of the strain gages could be deducted from the total flight response, leaving only the aerodynamic responses from which loads could be derived.

It was planned to demonstrate this approach on one of the canards on the XB-70 aircraft. The canard was to be instrumented with strain gages and thermocouples and then flown to Mach 3. The measured thermal field at Mach 3 was to be applied to the canard in the laboratory which would result in corrections which could be applied to the flight data. This plan went awry when the XB-70 airplane that was to be used was lost in an accident in 1967. The single remaining XB-70 airplane was retired shortly thereafter when the program was terminated.

Shortly after the XB-70 accident, several YF-12A aircraft became available to the NASA Flight Research Center for research activities. One of the aircraft was identified for flight loads measurement research. The bold approach was adopted. This approach used the entire airplane as the test specimen; therefore, the entire airplane was instrumented with strain gages and thermocouples, flown to Mach 3, and heated in the ground-based infrared-heating laboratory to obtain corrections for the strain gages. The remainder of this paper tells the story of an unusually complete and unique scientific program. Partly by coincidence and partly by design, this program simultaneously brought together an exceptional aircraft, a powerful ground-based heating laboratory, the computational tools of the day, and an appropriate technical group.

YF-12A LOADS MEASUREMENT SCENARIO

The primary objective of the YF-12A loads and structures effort was to measure the aerodynamic forces on the airplane in flight with calibrated strain gages. The sustained Mach 3 cruise capabilities along with other advanced design features rendered this airplane the most challenging choice. The

thermal environment is appropriately depicted in figure 1 where surface temperatures up to 600 °F are seen (ref. 10). Bearing this thermal environment in mind, extensive onboard instrumentation, such as strain gages, thermocouples, and deflection measuring targets and cameras, was installed within the structure. An extensive loading system was designed and built to calibrate the installed strain gages. An even more complex heater system was also designed and constructed to simulate the thermal environment which the structure experienced during flight. The installed sensors, loading, heating, and flights provided the baseline information from which the research effort evolved.

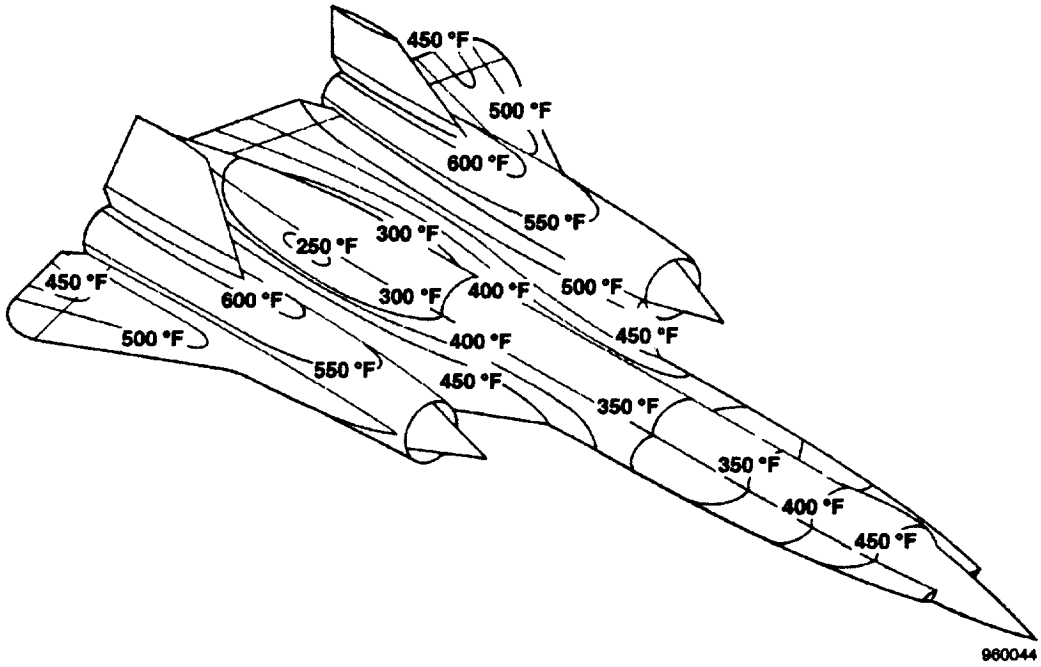

Figure 1. The YF-12A aircraft with upper surface temperature contours (ref. 10).

It was realized that related technology areas should be explored in association with the basic flight loads program. In addition to the primary objective, many less visible, but just as important, activities were achieved with significantly less effort and resources. The generation of extensive laboratory temperatures, stresses, and deformations with respect to a heated and loaded airplane provided an opportunity to study many subtechnologies, such as verification of codes associated with load equation derivations, deformation predictions, stress calculations, and temperature predictions. Other technological studies involved sensor technology with regard to high-temperature strain gages and thermocouples, in-flight and laboratory structural deflection measuring systems, aircraft loading technologies, infrared-heating technology, and data acquisition and control science.

Basic Airplane Structure

Figure 2 shows the structural skeleton of the YF-12A airplane (ref. 11). The fuselage structure and engine nacelles are formed as a ring-stiffened structure. The wings are constructed from multiple spars and ribs. The aircraft structure was fabricated primarily from several titanium alloys.

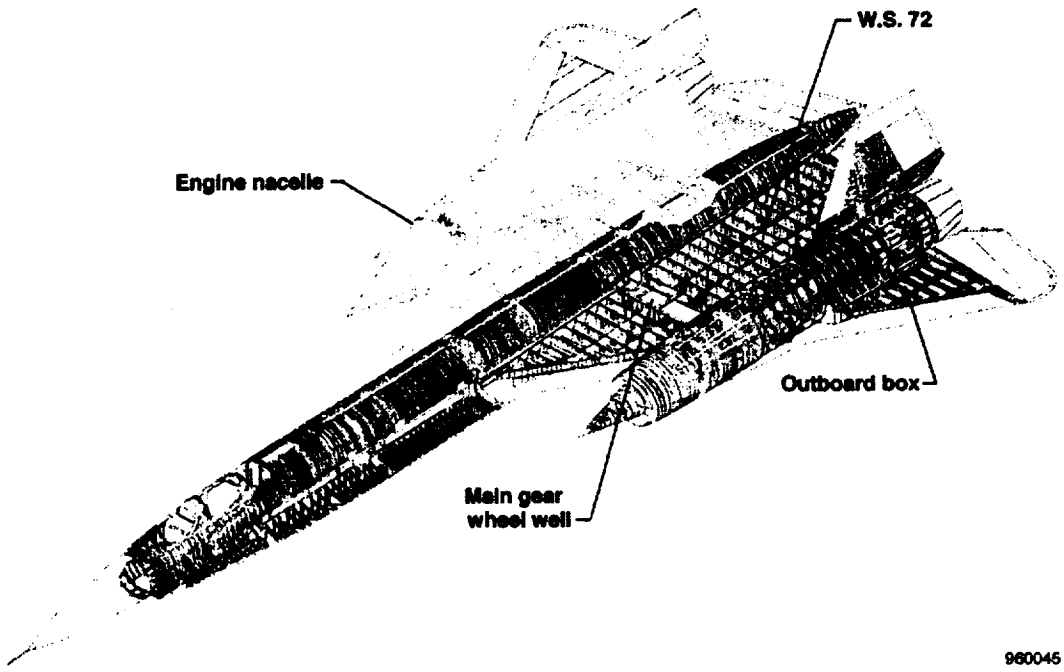

Figure 2. Structural skeleton of the YF-12A aircraft (ref. 11).

Strain Gage Response to Load

An aircraft that flies at speeds sufficient to result in significant structural heating has special problems associated with attached strain gages and the associated structure. Figure 3 shows two of these effects. The hot strain gage output may indicate a zero shift or what may be called a thermal shift which can result from two sources. The shift (i.e., from A to B) may result from the apparent strain of the strain gage which arises from the mismatch of the thermal expansion characteristics of the strain gage material and

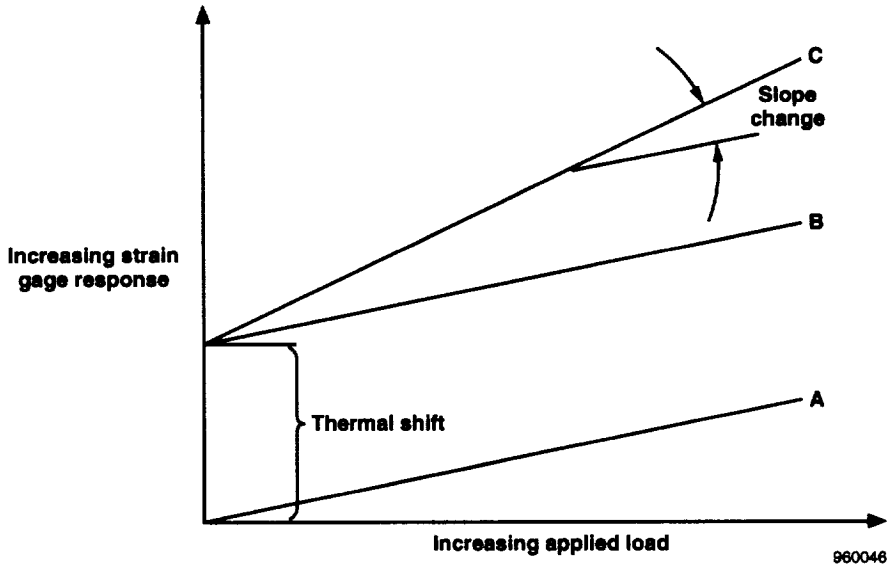

Figure 3. Primary elevated temperature problems associated with strain-gaged aircraft.

the material to which the strain gage is attached, for example, the substrate. If the temperature field of the structure is nonuniform, then a thermal stress field results in the airplane structure which also is sensed by the strain gages as a shift.

The second effect is seen as a slope change, such as from B to C (fig. 3). A change in the response of the strain gage to loads (slope change) may be caused by several factors. The increased temperatures may be sufficient to reduce the modulus of elasticity of the structural component. This reduction in elasticity would increase the response of the strain gage to the load. The higher operating temperature of the strain gage may also change the response of the strain gage to load (gage factor). The third manner in which the slope could change results from actual load path alterations because of differential stiffness changes among the spars and ribs.

Thermal Calibration of the YF-12A Airplane

Any attempt to computationally account for individual thermal effects would have resulted in an extremely large, and perhaps impossible, effort. The idea of an experimental correction to the flight data was very attractive because no complicated or uncertain computations were required. Figure 4 shows the basic approach to using the thermal calibration (ref 12). The value of the thermal correction (thermal load) to the strain gages was obtained by applying the flight-measured temperatures of the aircraft to the structure on the ground using an infrared heating test. Once the thermal correction (load) is known, then the flight test data can be corrected by deducting the thermal part of the load from the total load. The remainder is the response of the strain gage to the aerodynamic part of the load.

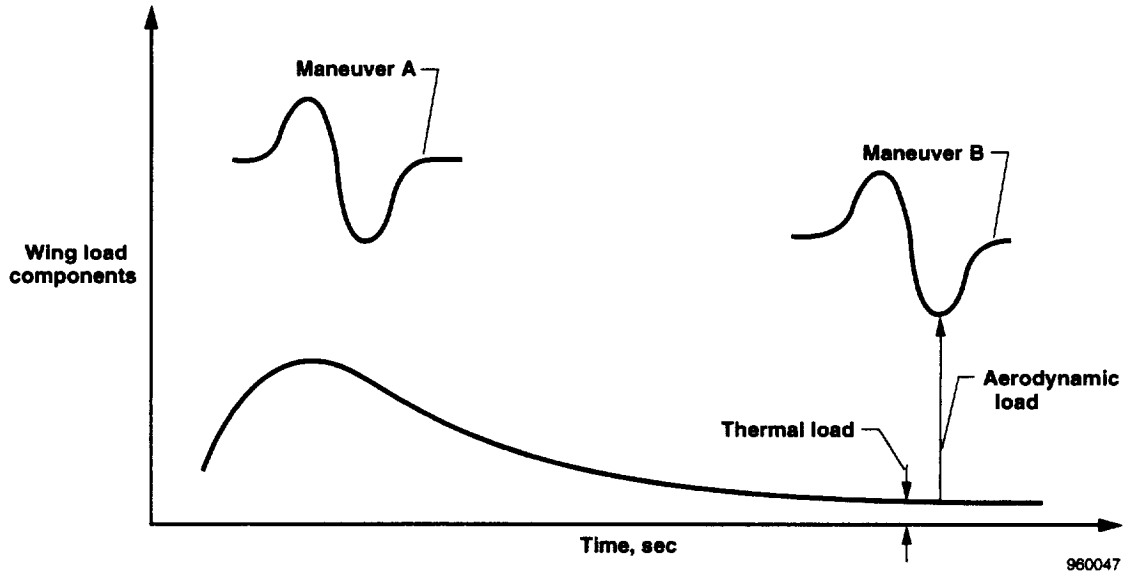

Figure 4. Aerodynamic and thermal components of load relative to flight profile (ref. 12).

Structural Details

The YF-12A airplane designer incorporated several features within the structure to provide relief from thermal expansion. Figure 5 shows the general nature of the wing structure (refs. 10 and 13). Stand-off clips were included to minimize the transference of thermal expansion to the substructure from the hot

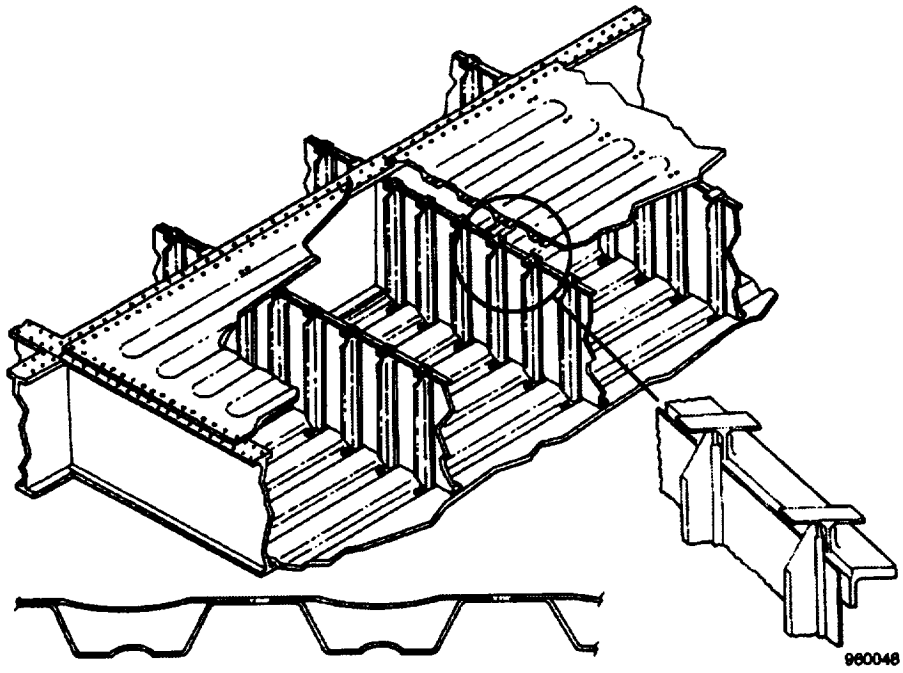

Figure 5. Thermal expansion relief on the YF-12A wing structure (refs. 10 and 13).

skins. These stand-off clips also minimized the heat conduction paths to the substructure. The skin panels also included significant beading to allow flexible thermal expansion rather than thermal stress build up.

Note the complexity of the YF-12A structure. Computer models will be introduced later in the paper from which computational predictions are compared to experimental results.

Figure 6 shows selected details of the wing structure (ref. 14). With such drastic differences in detail, the modeling idealizations are not an easy task.

HEATING THE YF-12A AIRPLANE

Heating the YF-12A airplane was a challenging endeavor. The airplane required considerable preparation before laboratory heating. Note that this airplane was to undergo extensive loading and heating in a laboratory and then be reinstated as a flying airplane, so the tests did not involve what could be considered an ordinary test specimen. The major concern with heating the airplane in the laboratory was the possibility of an explosion. The JP-7 fuel used in this airplane can autoignite at temperatures slightly over 400 °F. Many fuel tanks exist throughout the fuselage and wings, and a great deal of insulation is also installed throughout these areas. These fuel tanks had significant leaks; hence, the insulation in many areas contained residual fuel. The explosive hazard was a serious concern, and appropriate precautions were taken.

The general thermal environment of the YF-12A structure involved a hot skin with a cooler substructure. In some locations however, the substructure was hotter than the skin area. These locations were attributed to either heat from the engine or hot boundary-layer air entering the structure through drain holes in the skins. The heating profile in figure 7 typifies a Mach 3 flight where an acceleration period results in increasing skin temperatures (ref. 10). Such temperatures rapidly come to an equilibrium

situation when the Mach 3 cruise condition is reached. The substructure lags the skin temperatures at first, but late in the flight the substructure reaches near steady state. The time history of figure 7 gives the reader a feel for the nature of the heating simulation required.

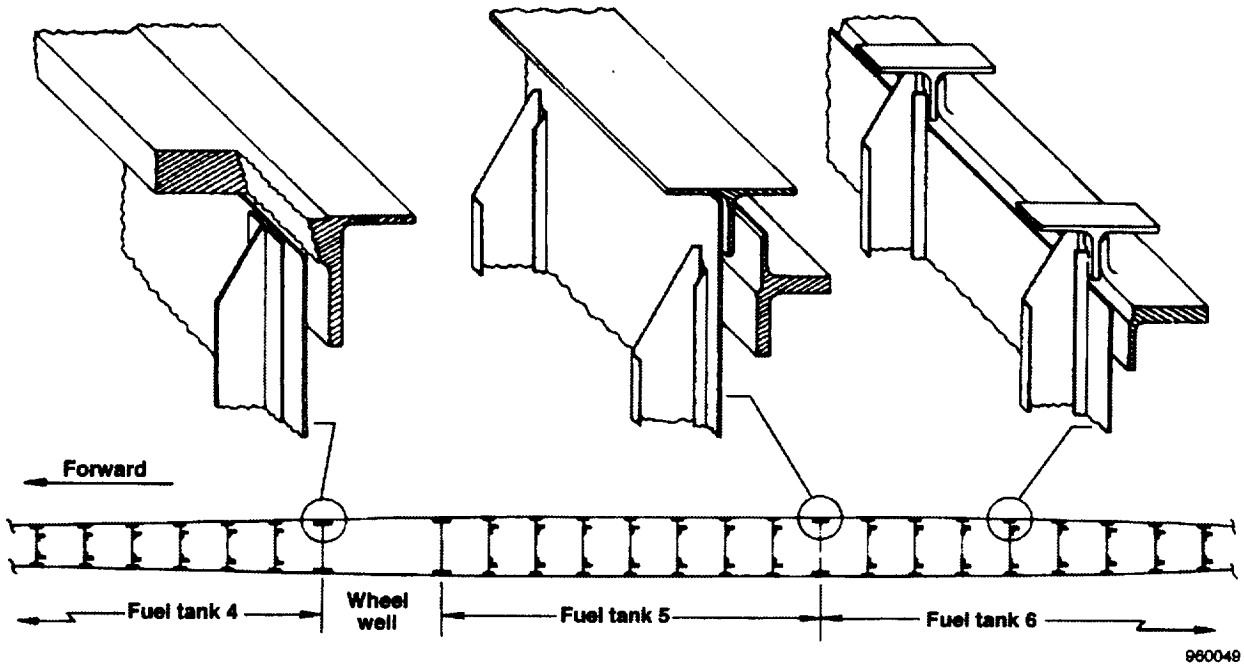

Figure 6. Difference in substructural detail (ref. 12).

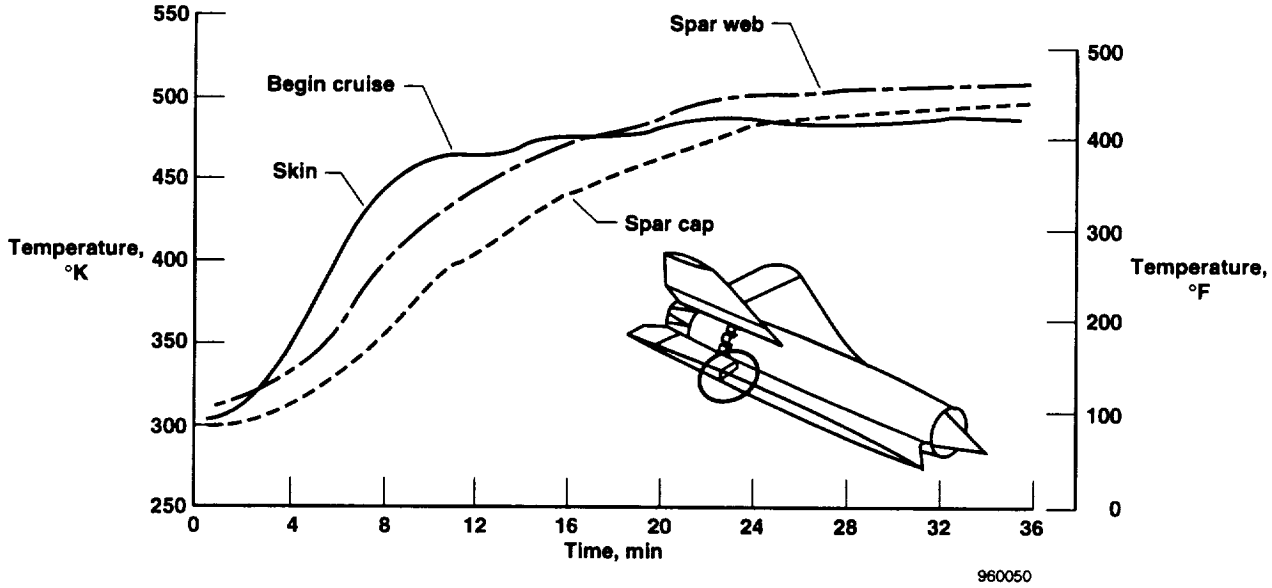

Figure 7. Time history of typical wing spar temperature distribution (ref. 10).

Heater Configuration and Control Zones

The heating of the airplane was formulated around five primary heater areas (fig. 8). These heaters were arranged for ease of removal from the airplane and to facilitate inspection and repair. One large heating system built on rollers was used to heat the aft section of the airplane. The middle of the airplane was heated with lower heaters on rollers and two upper sections which could be moved up and down similar to a drawbridge. The forebody was heated with two systems which rolled into heating position from the side.

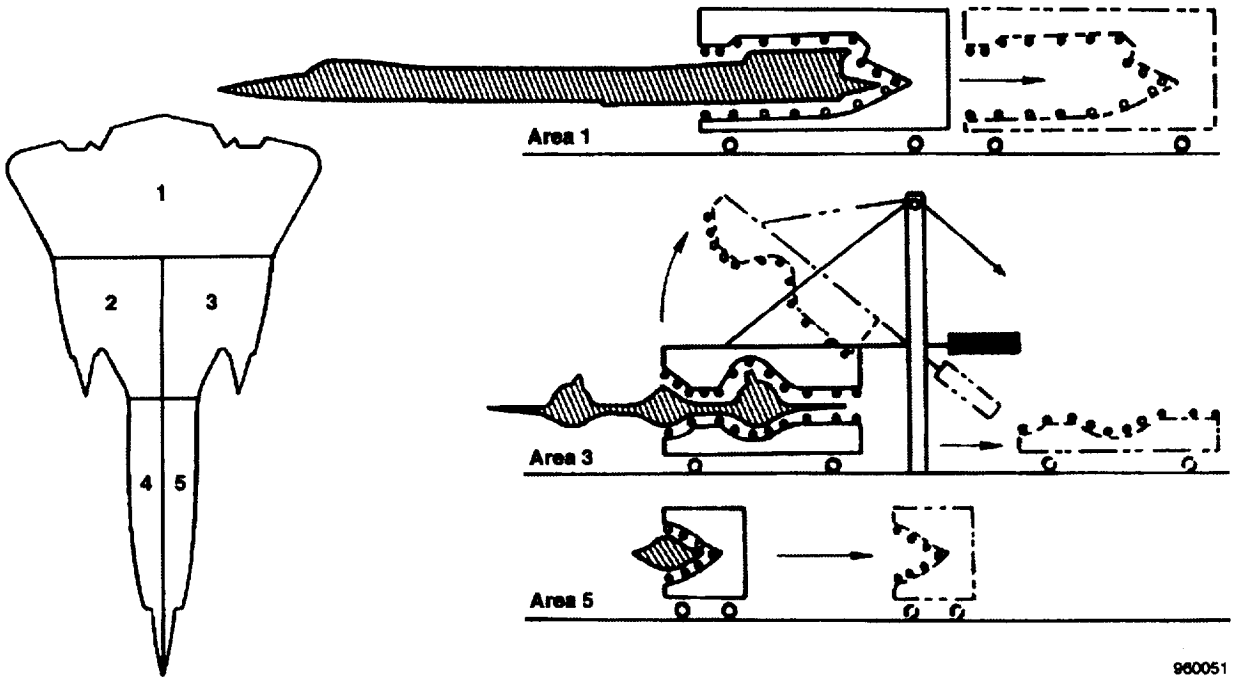

Figure 8. Heater panel configuration.

The five primary heaters were further subdivided into many heater control zones. Each was controlled by a surface thermocouple. The required zonal temperatures were achieved by controlling surface temperatures on the airplane at approximately 600 locations on one symmetrical half of the airplane. Duplicate zones on the opposite side of the airplane were controlled in parallel. Surface thermocouples were installed on selected duplicate zones. Temperatures obtained from these thermocouples were used to verify that the temperatures on the opposite side of the airplane agreed with the corresponding control zone temperatures. Figure 9 shows the distribution of heating control zones for the lower side of the airplane, and figure 10 shows the typical heater and control zones (ref. 13).

A nacelle heater was also included to simulate the exact three-dimensional temperatures in the engine area. Figure 11 shows a sketch of the nacelle heater (ref 14).

One-half of the forebody heater is shown in the foreground of figure 12 in a retracted position. The background shows the upper middle heaters in the raised position. A somewhat clearer view of the upper

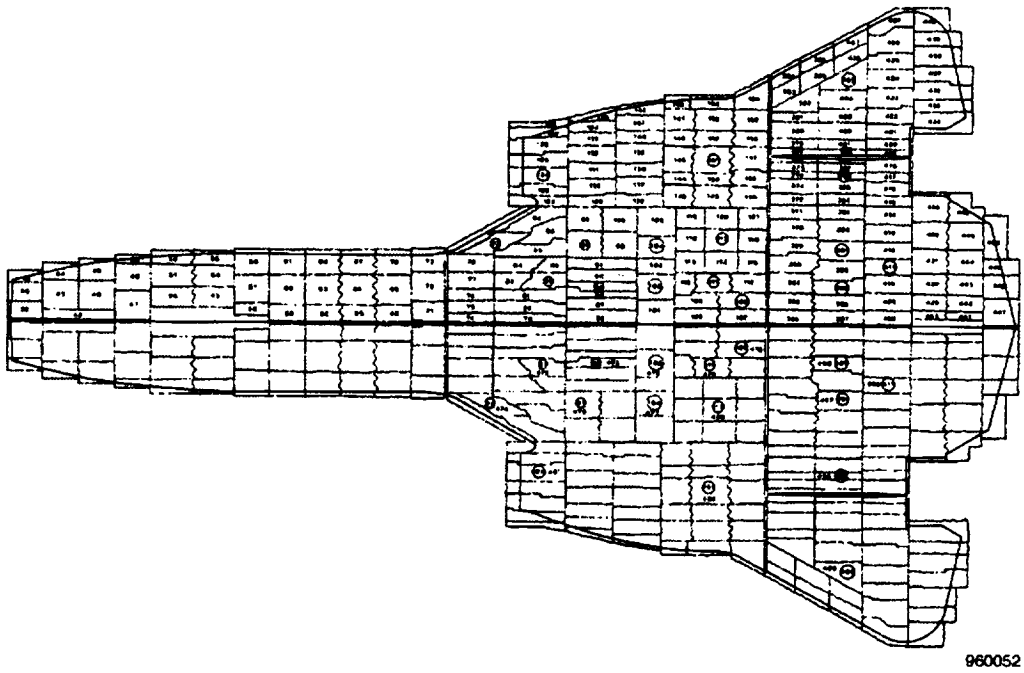

Figure 9. Distribution of lower surface heater control zones (ref. 13).

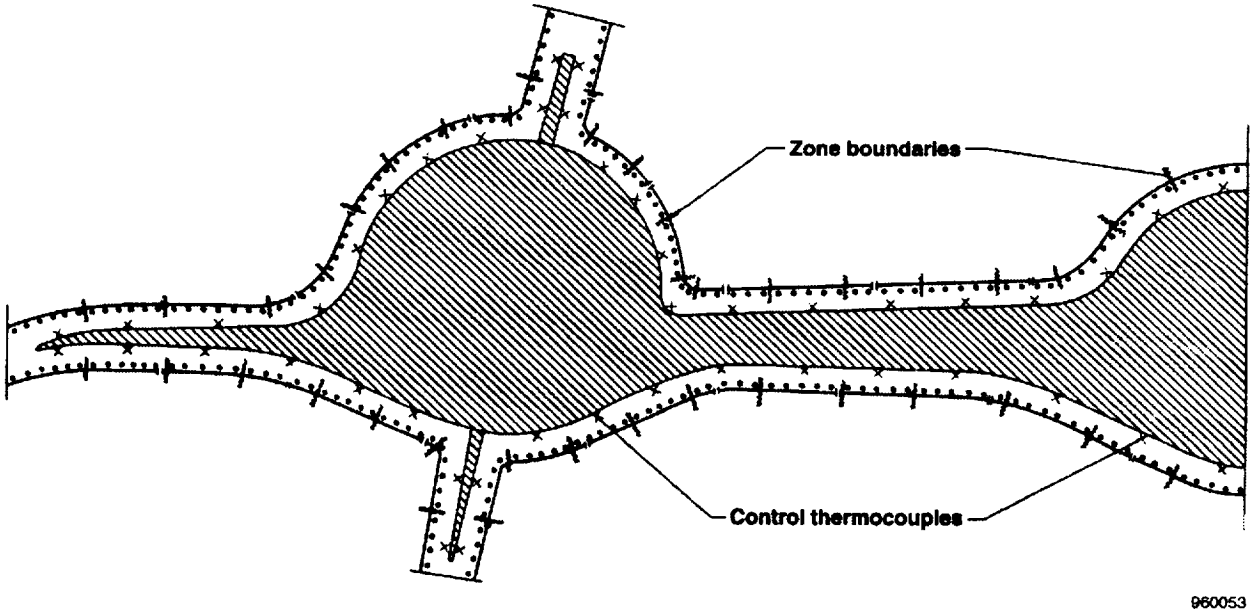

Figure 10. Typical zoning arrangement and control thermocouple location (ref. 13).

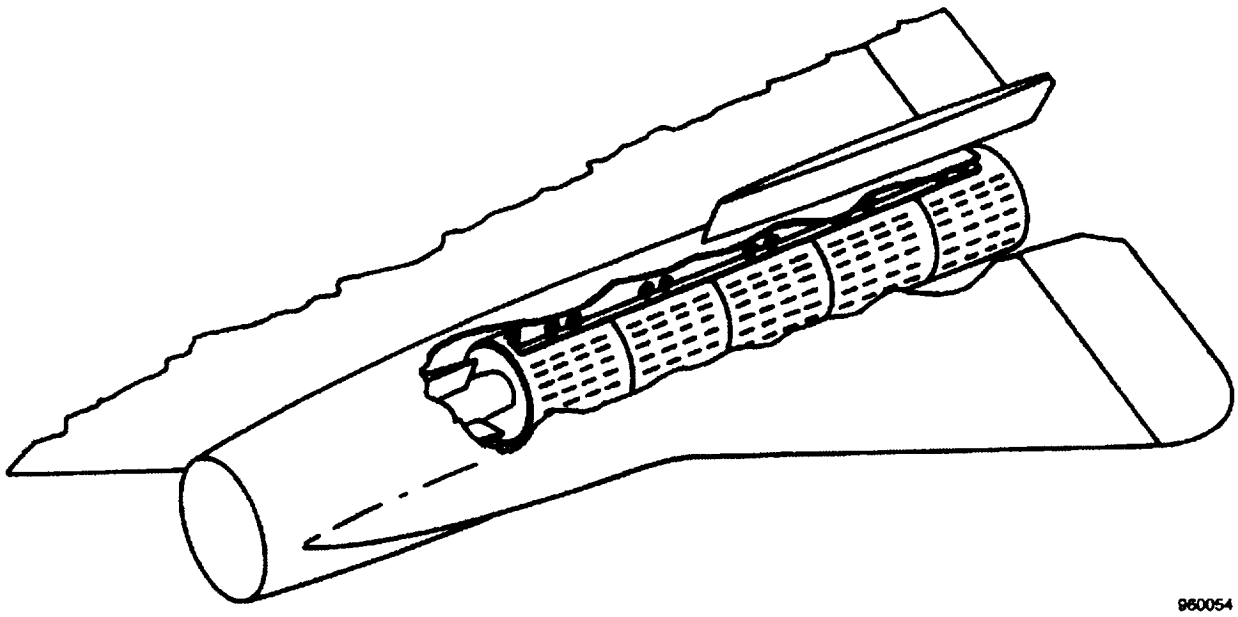

Figure 11. Nacelle heater location (ref. 14).

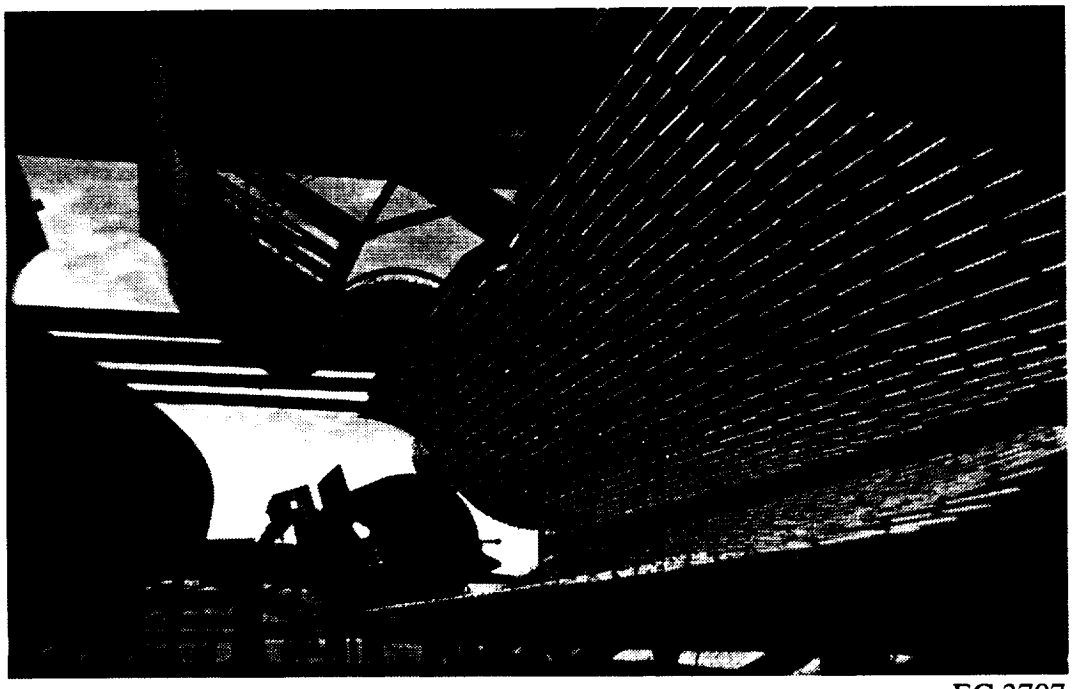

EC 3707

Figure 12. Front heater and upper middle heater in retracted position.

middle heater is shown in figure 13. In figures 12 and 13, the lamps are undergoing checkout tests. Figure 14 shows the aft heater in the retracted position. Figure 15 shows the nacelle heater during lamp installation. Figure 16 shows the aft heater and the middle heater in position to heat the airplane. References 13–15 provide an extensive description of the details of the heating and the control of the heating processes.

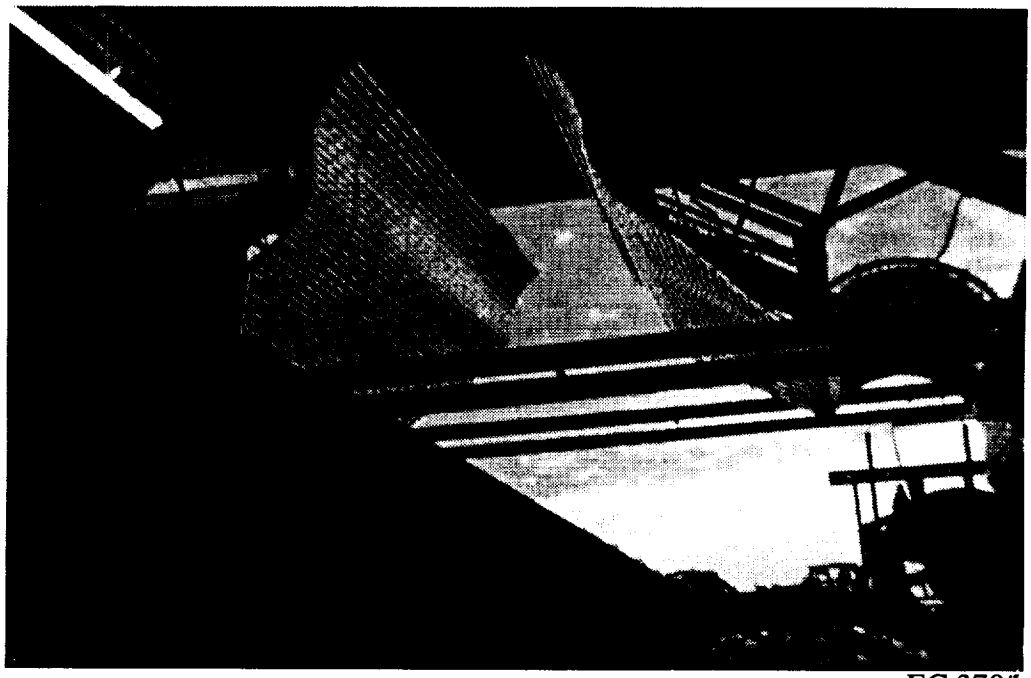

EC 3705

Figure 13. Both sides of the upper middle heater.

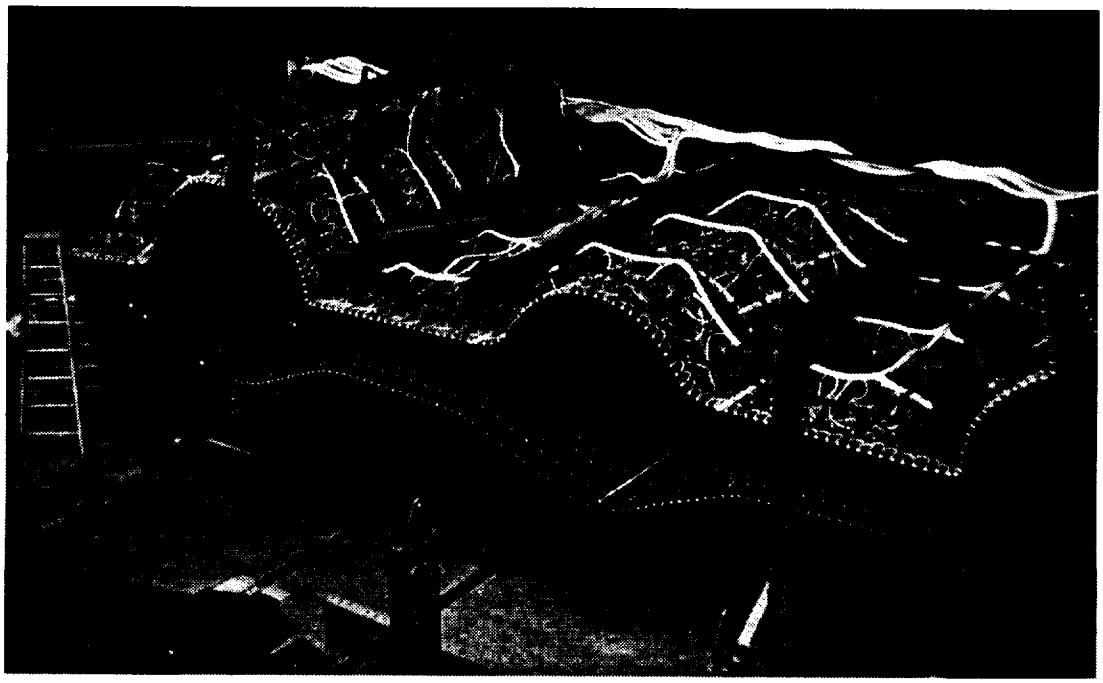

EC 3717

Figure 14. Rear heater in retracted position.

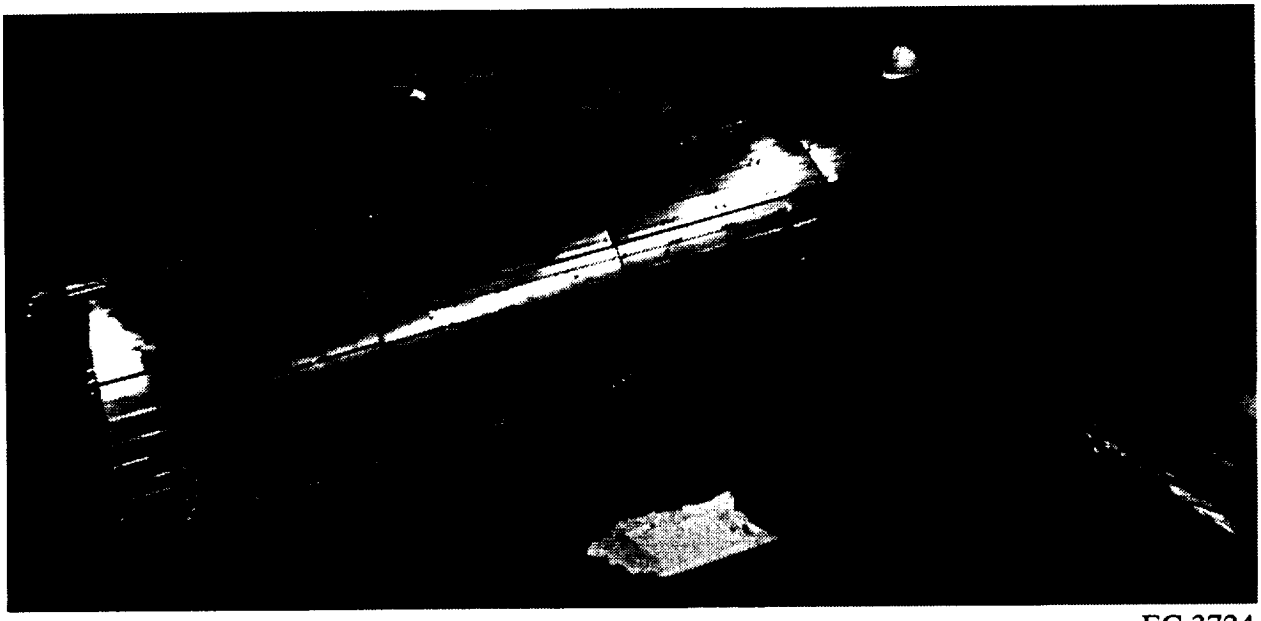

EC 3724

Figure 15. Nacelle heater.

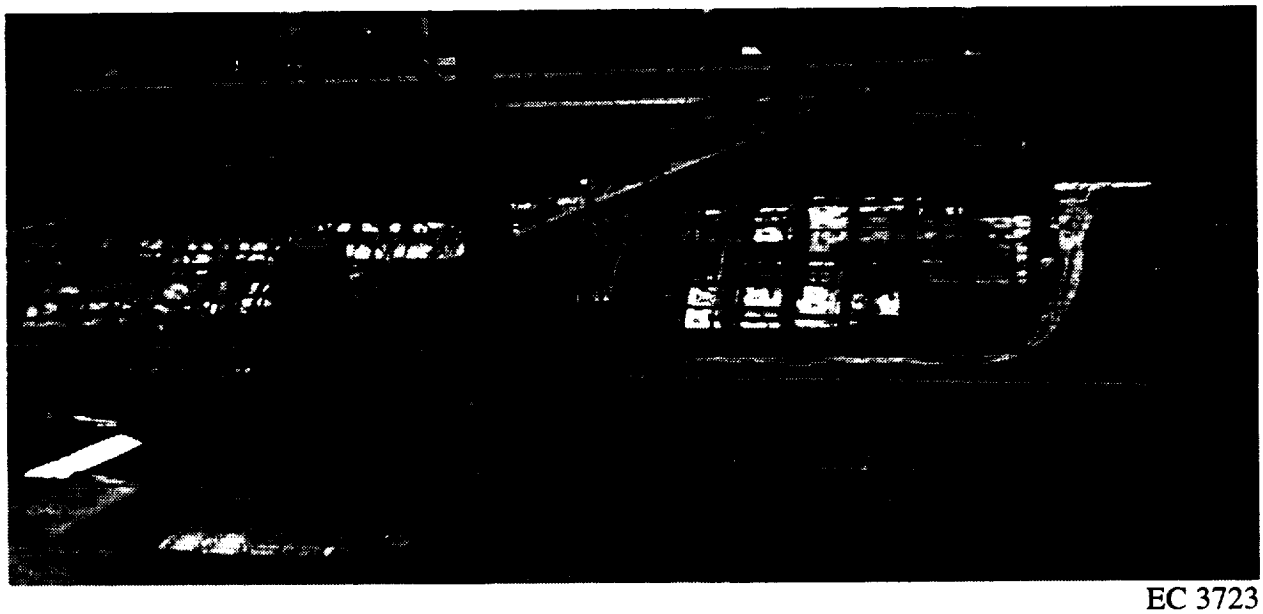

EC 3723

Figure 16. Rear and middle heaters in the aircraft heating position.

Airplane Preparation for Heating Tests

Because the YF-12A airplane would be returned to flight status following the heating tests, extensive preparation was required before the heating simulation could be performed. The vertical tails, nose cone, and engines were removed for the heating test (fig. 17) (ref. 14). The presence of these components has no affect on the ultimate result of the thermal calibration. The fuel used by this airplane autoignites when temperatures exceed 400 °F; therefore, special precautions were required to prevent an explosion during

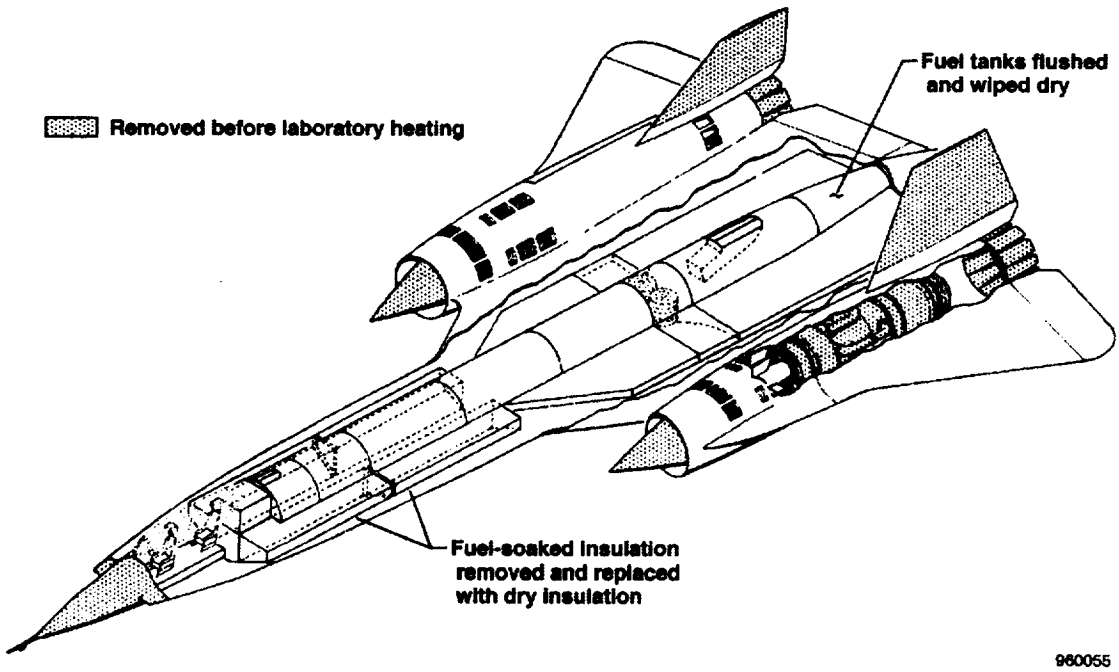

Figure 17. Airplane preparation for laboratory heating tests (ref. 14).

the laboratory heating. The fuel-soaked insulation was removed and replaced with dry insulation. The fuel tanks were flushed with a solvent and wiped dry. During the heating test, these tanks were purged with gaseous nitrogen, and the oxygen content was monitored.

Results of the Heating Simulation

Figure 18 compares the flight-measured temperatures (symbols) and the laboratory heating simulation (lines) at three forebody locations (ref. 14). Upper and lower fuselage stiffener temperatures and the temperature of the fuel tank skin are shown. The overall agreement between flight and simulated temperatures is good. For the upper fuselage, however, the simulation under predicted the flight data by 15° to 20° F. This difference results from using radiant heating to simulate aerodynamic heating. Because of the basic difference in the way heat is transferred, the radiant heating rate in areas of increased structural mass will be lower than the aerodynamic heating rate (ref. 7).

Figure 19 shows additional comparisons at three points in the aft portion of the airplane (ref. 14). The laboratory heating resulted in close agreement at the nacelle skin and dry bay skin areas. Laboratory temperatures at the fuel tank skin exceed the flight temperatures. This disparity was caused by the difference in amounts of fuel. An in-flight airplane carries fuel; whereas, this laboratory test was conducted with a dry fuel tank. The fuel acts as a thermal heat sink. The simulation and flight values converge after the fuel has been expended. Strain gage data from flight in this area could not be corrected until the laboratory and flight temperatures converged, and a meaningful correction could be established.

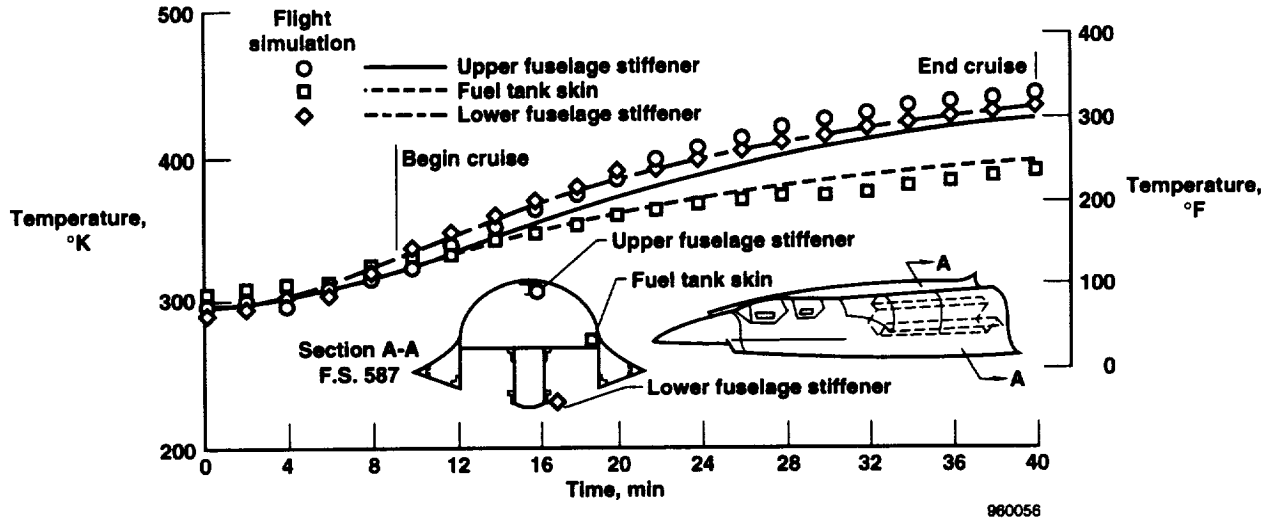

Figure 18. Results of the Mach 3 heating simulation in the forebody area (ref. 14).

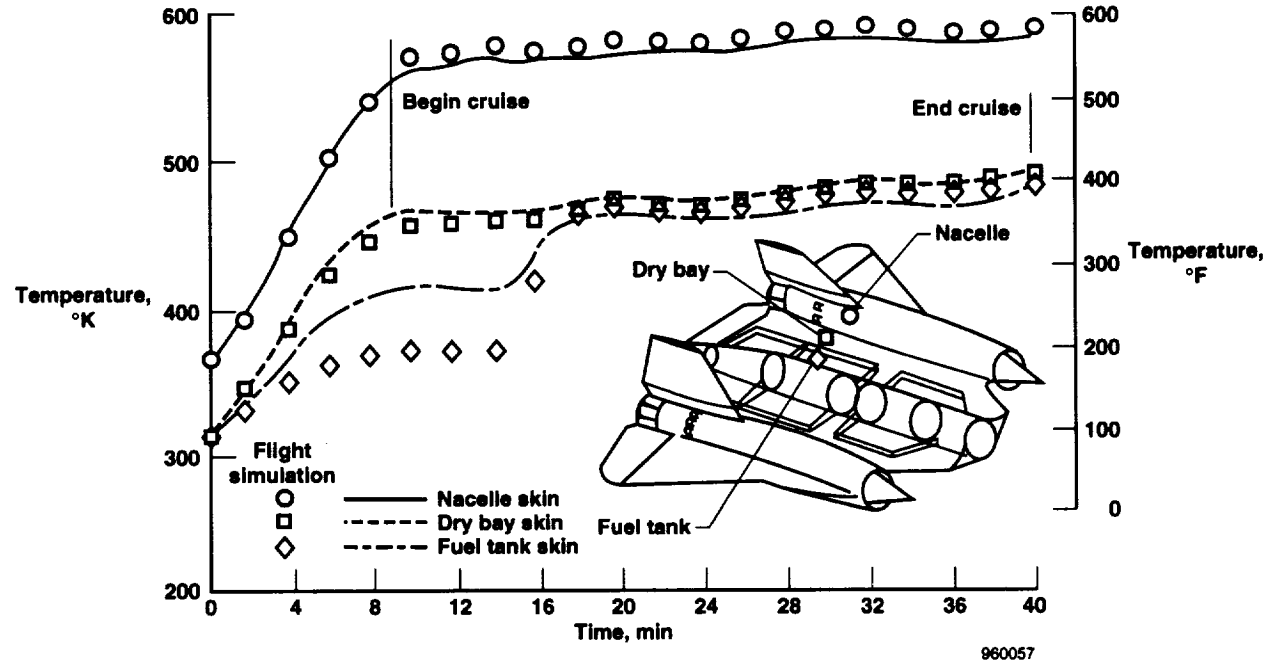

Figure 19. Results of the Mach 3 heating simulation in the skin area (ref. 14).

The results shown in figure 20 further illustrate the difficulty of duplicating the skin temperatures in the fuel tank areas (ref. 14). A single control zone was used to heat the fillet and fuel tank skin. This zone also indirectly heated the spar cap. Because the temperatures of the fillet and fuel tank were so different during the first 16 min of the flight profile, duplicating both temperatures was impossible. Smaller control zones could have solved this problem, but reducing these zones was not possible for the test. Consequently, in an attempt to produce the correct heating load at the spar caps and corresponding strain gages in these areas, the control zone temperatures were programmed to duplicate the average measured temperatures of the fillet and fuel tank skin. This approximation to the surface heating proved quite successful as indicated by the good agreement between the measured and simulated spar cap temperatures (fig. 20).

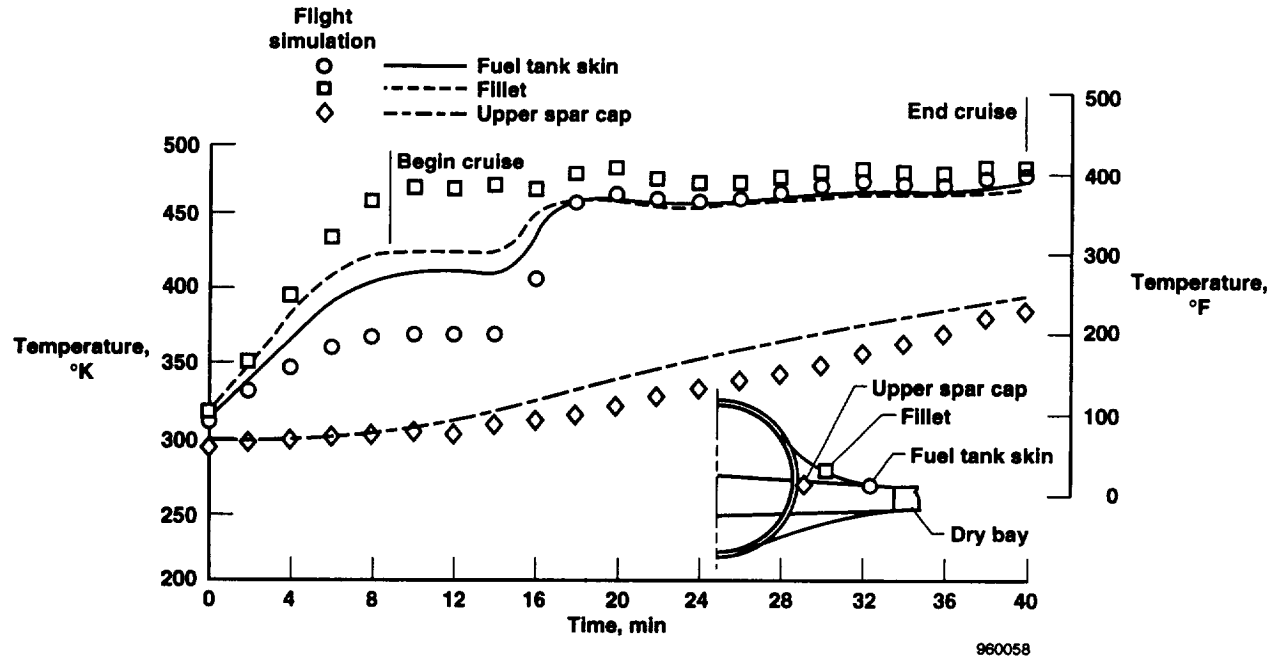

Figure 20. Results of the Mach 3 heating simulation in the skin, fillet, and spar cap (ref. 14).

Radiant Heater Augmentation with Hot Nitrogen Gas

In areas where internal heat sources existed, such as from engine heat or hot gages entering through drain holes, special heating measures were required. In the area shown in figure 21, the initial simulation (solid line) was quite in error (ref. 14). The first attempt to correct this problem involved preheating the area with the radiant heaters (dashed line). This preheating approach did not correct the problem. In the long run, however, by injecting heated gaseous nitrogen into the substructure, an acceptable simulation was achieved.

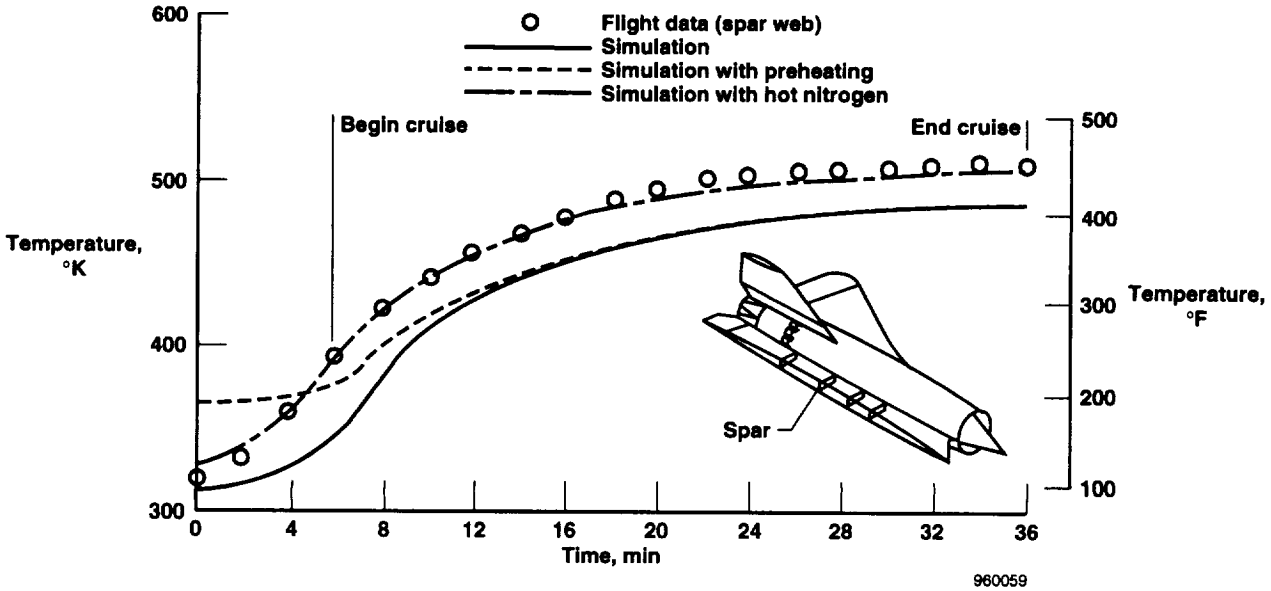

Figure 21. Results of radiant heater augmentation with hot nitrogen gas (ref. 14).

Figure 22 shows the heating of the airplane. These tests were conducted late at night because of the anticipated power requirements. The heater system was much more efficient than expected, so the night tests were eventually discontinued, and this work was completed during the daytime.

EC 3708

Figure 22. Rear view of YF-12A airplane during a radiant heating test.

YF-12A LOAD CALIBRATION

This section describes the laboratory mechanical loading of the YF-12A, the manner in which the loads were applied to the aircraft, and the method of restraining the aircraft. Two structural models are presented, and comparisons of predicted and measured influence coefficients, stresses, and deformations are made.

Wing Loading and Strain Gages

The basic approach in a wing strain gage calibration is to load the wing at a series of chord and span locations, record the strain gage response to the grid of loads, and develop loads equations which relate applied loads, such as shear, bending and torque, to strain gage outputs (ref. 16). References 11 and 17 provide additional information specifically relating to the load calibration of the YF-12A wing. The strain gages in the YF-12A wing area were calibrated for load to be the upward loading of the wing from the bottom. An overhead restraining system, consisting of loading jacks, was programmed to maintain a constant gear load (figs 23 and 24) (ref 11). The landing gear rested on roller-bearing plates which allowed translation in the plane of the wing. Position transducers provided information about the out-of-plane deformation of the wing during loading (fig. 24).

Figure 25 shows two of the loading cases (ref. 18). The top case involved loading the engine nacelle upwards and reacting the load with overhead jacks to maintain a constant gear load. The bottom case involved loading the outboard wing at two points and again reacting the loads overhead to maintain a constant gear load. The plan included measuring loads at three outboard wing stations (W.S.). Extensive strain gage instrumentation was located at W.S. 35, 111, and 215 (fig. 26) (ref. 11). The strain gage instrumentation consisted of four active arm strain gage bridges.

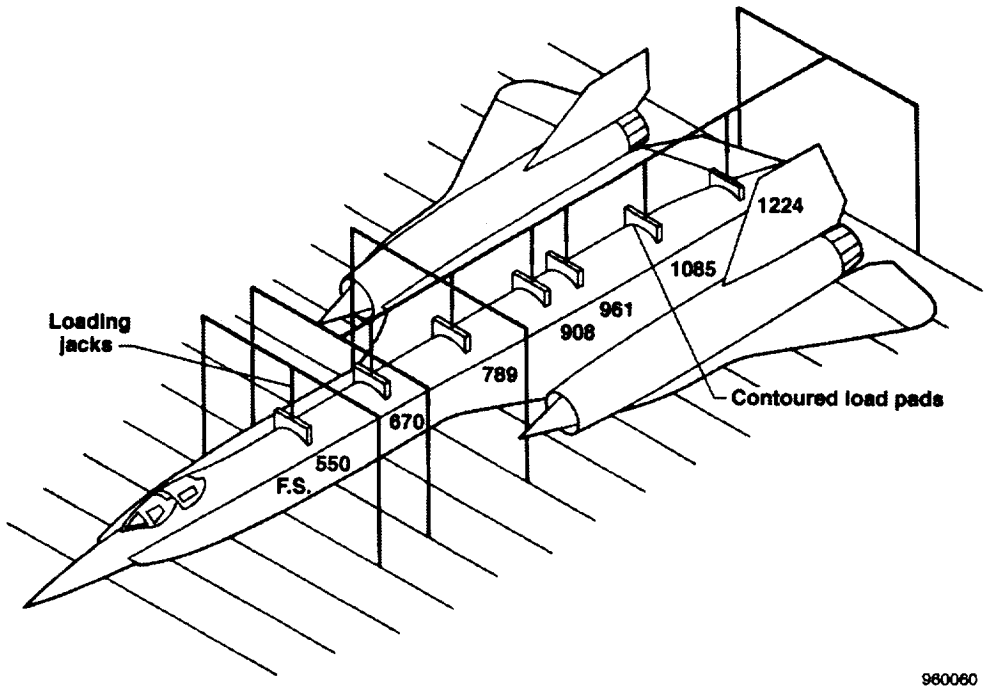

Figure 23. Fuselage reaction fixture for load tests. (ref. 11).

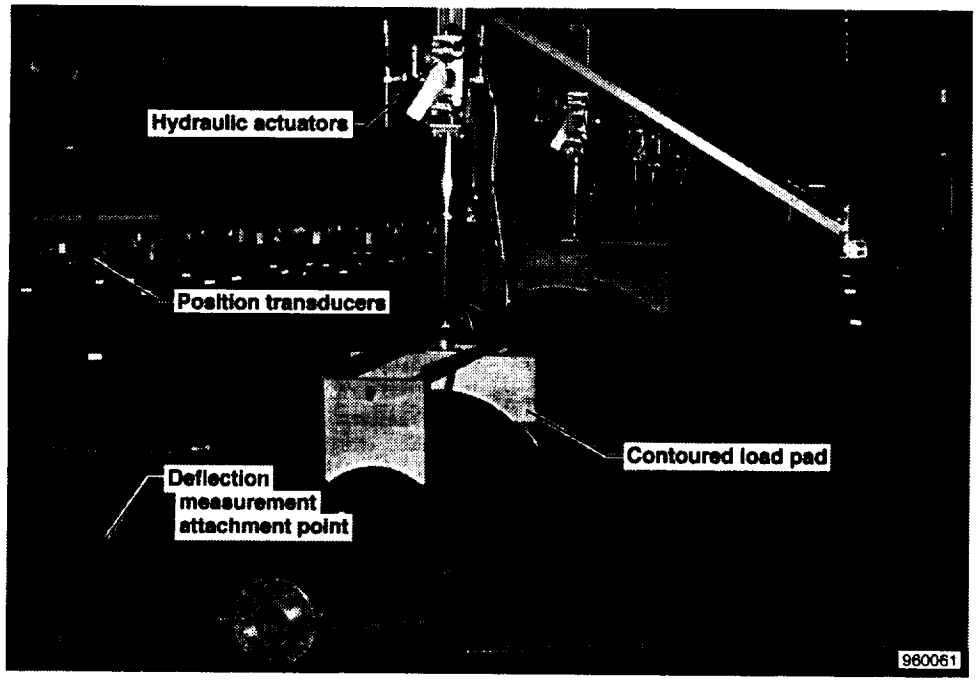

Figure 24. Fuselage reaction and deflection measurement system.

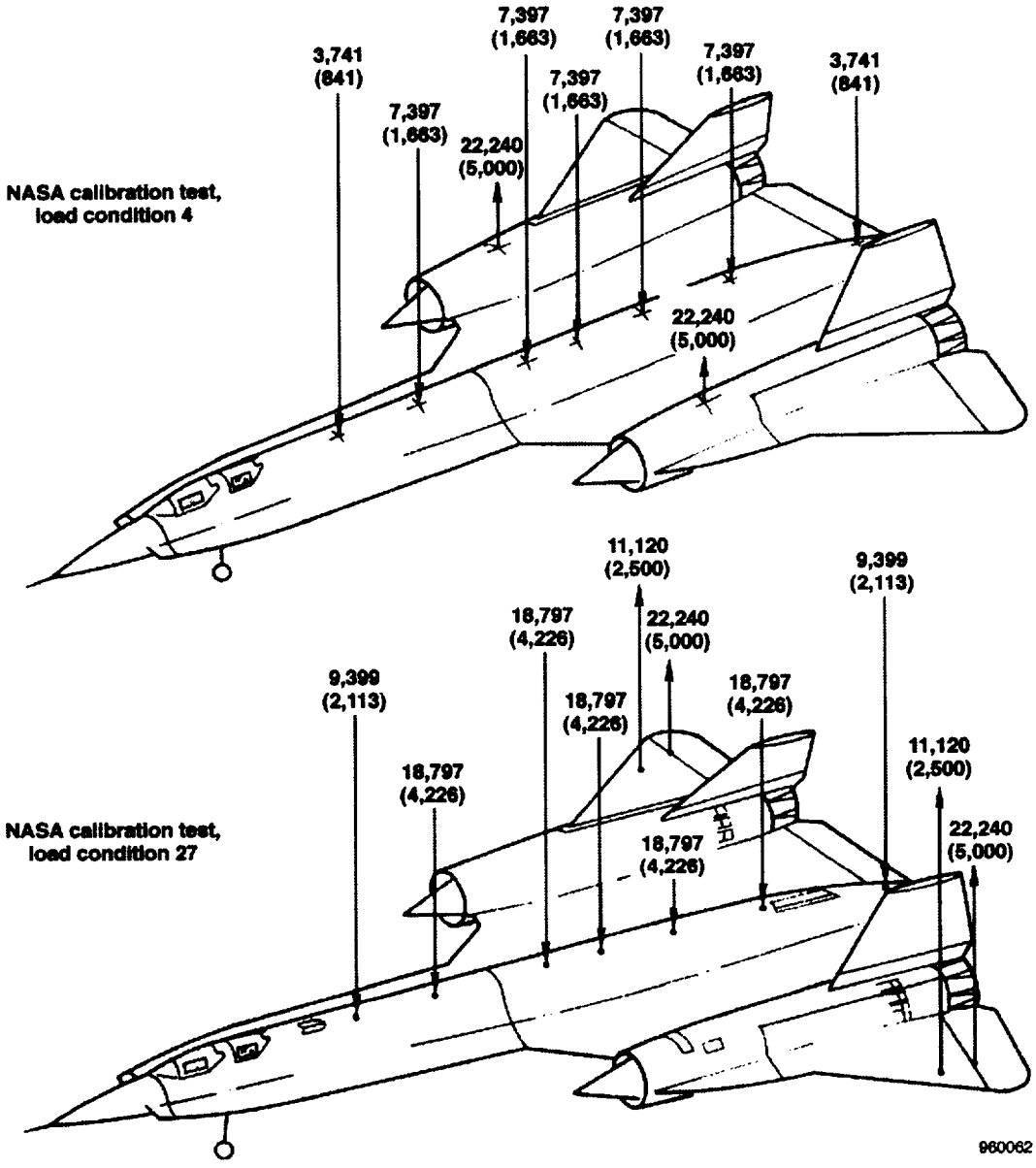

Figure 25. Typical point load calibration conditions (loads in newtons, lb) (ref. 18).

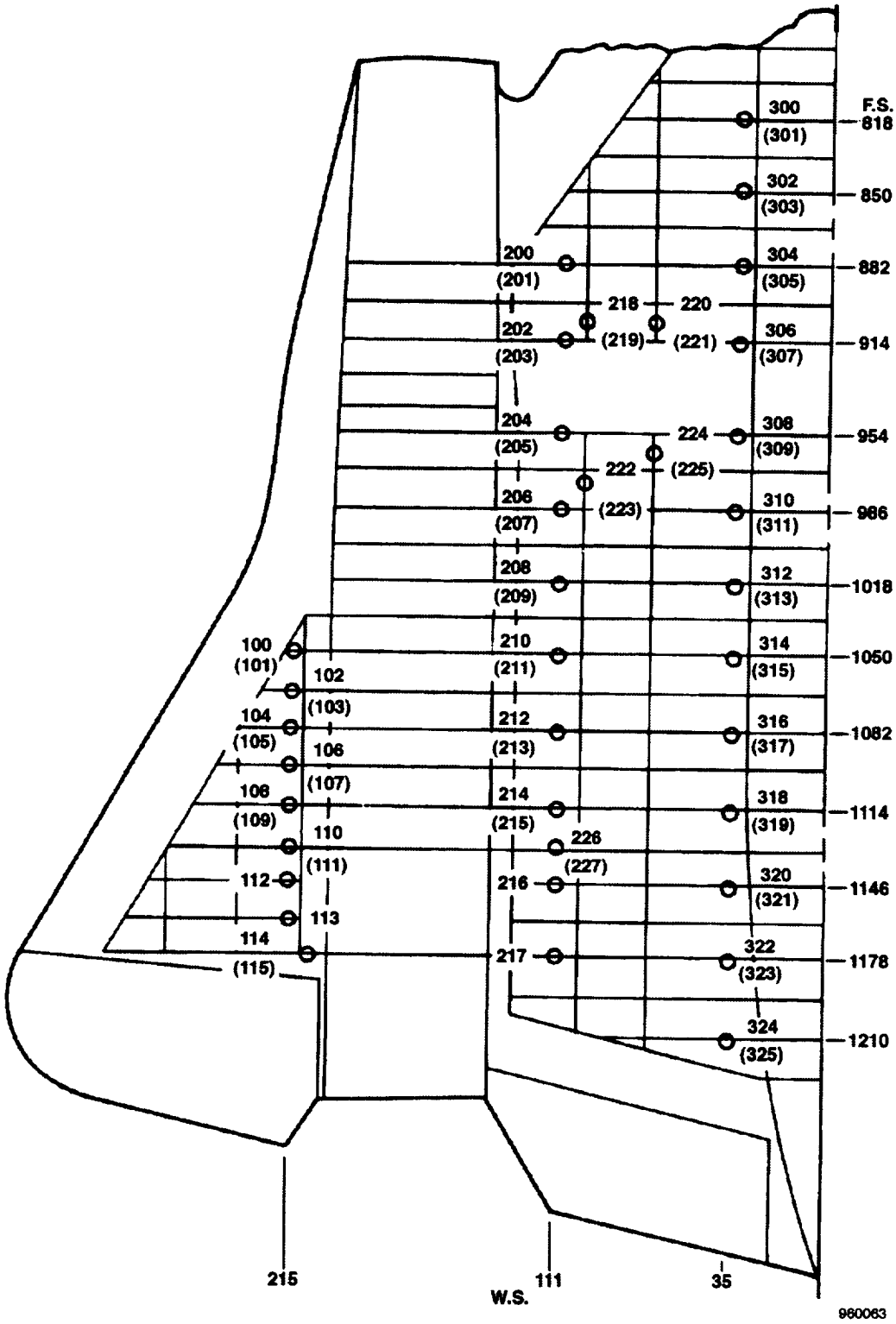

Figure 26. Strain gage bridges on YF-12A wing. Numbers in parentheses identify bending bridges. Numbers without parentheses identify shear bridges (ref. 11).

Comparison of Measured and Computed Stresses

Load equations relating aerodynamic forces to strain gage bridge outputs are derived from the load calibration of the aircraft. Influence coefficients (strain gage response divided by load) are calculated from the results of the laboratory load calibration. Influence coefficient plots that show the influence of a unit load in the span and chord direction. These plots are frequently used as an aid in identifying which strain gage bridges to use in various load equations. Because extensive experimental data were generated, two structural computer models were developed for use in conducting a general evaluation of the state-of-the-art in computing strains. The first avenue of interest was directed toward developing a simple NASTRAN model (ref. 19). This model could be used to determine how well computed influence coefficient plots would compare to plots generated from the laboratory data. Figures 27(a) and 27(b) show the simple model used to determine if influence coefficient plots could be predicted (ref. 20).

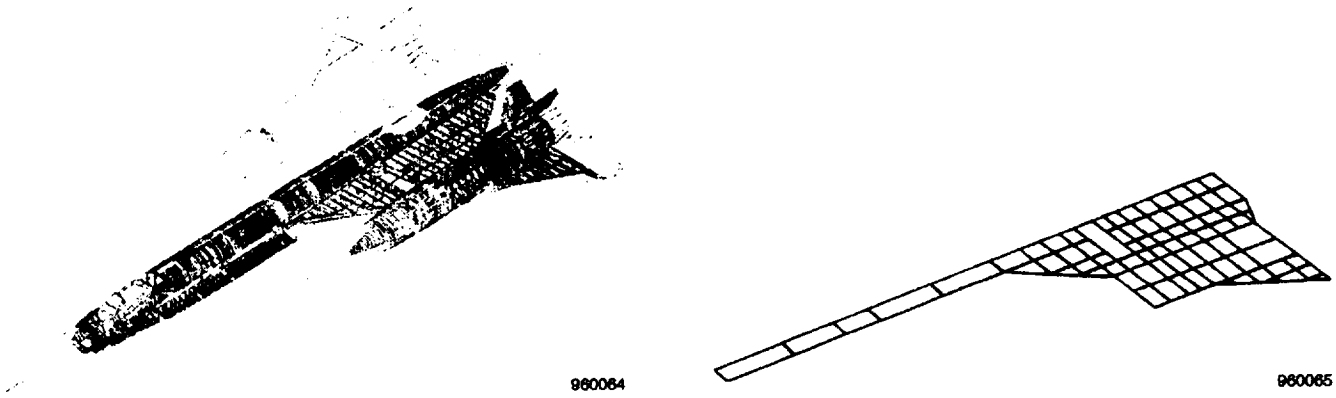

(a) YF-12A structural skeleton. (b) Simple structural model.

Figure 27. Structural skeleton of YF-12A airplane with simple structural model (ref. 17).

Figure 28 shows measured shear influence coefficient plots for three strain gage bridges on the YF-12A wing (ref. 20). The measured values are shown on the left, and the calculated values are shown on the right. The influence coefficient plots near the center and aft of the wing root correlate quite closely in terms of shape and magnitude. The strain gage bridge located forward, near the apex of the wing, correlates in influence coefficient plot shape but not in magnitude. This comparison shows promise of predicting influence coefficients using relatively simple models to represent delta wings.

Figures 29(a) and 29(b) show a comparison of measured and calculated influence coefficients for bending strain (ref. 20). Both the shape and magnitude of the measured bending moment influence coefficient plots for the YF-12A wing correlate with the calculated values. This result is typical for bending bridges.

Figure 30 shows an extensive NASTRAN model (ref. 18). This model was generated using rod, bar, and shear panel elements. In the 1960's, this model represented near state-of-the-art computer technology capacity. The model size required that the problem be run in six pieces. Figure 31 shows additional detail concerning the nature of the model (ref. 18). The diverse combination of elements results from the necessity to reduce the number of degrees of freedom.

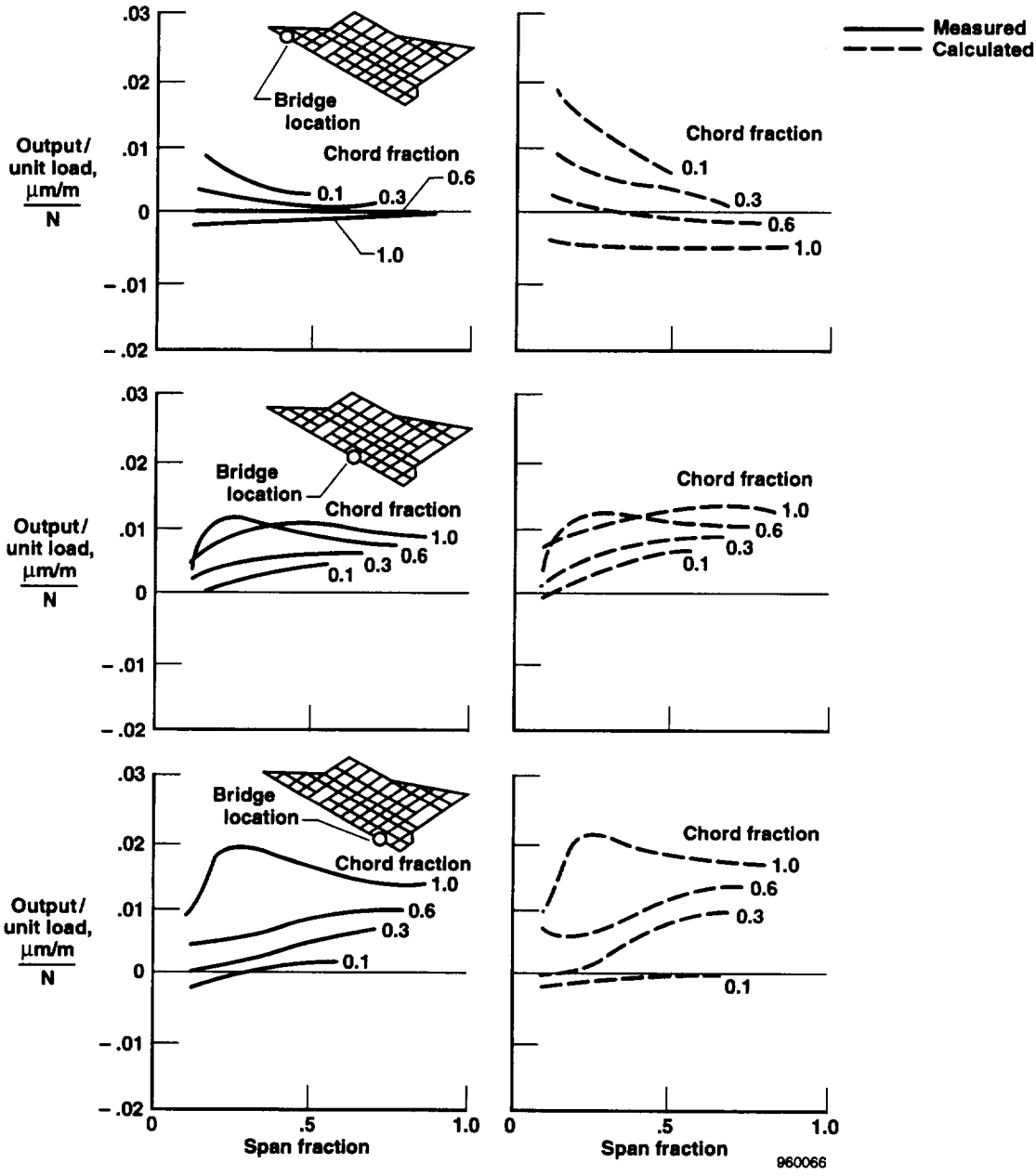

Figure 28. Comparison of measured and calculated influence coefficient plots for shear strain (ref. 17).

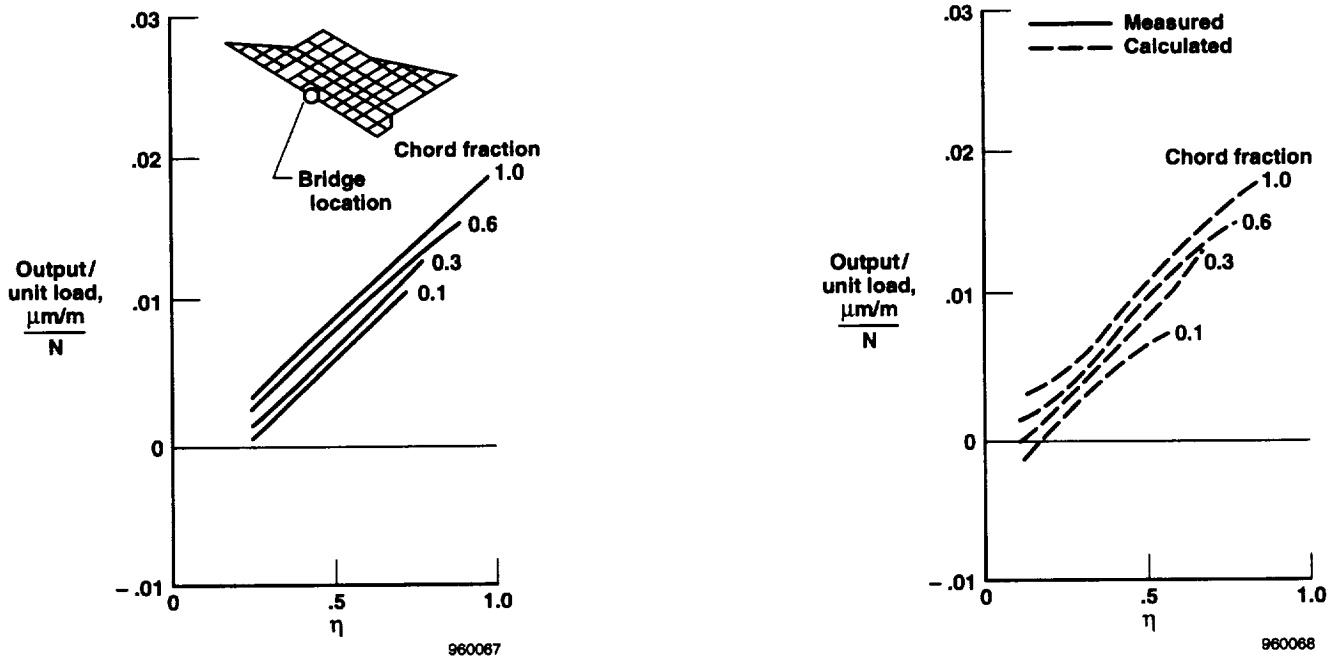

(a) Measured. (b) Calculated.

Figure 29. Comparison of measured and calculated influence coefficient plots for bending moment (ref. 17).

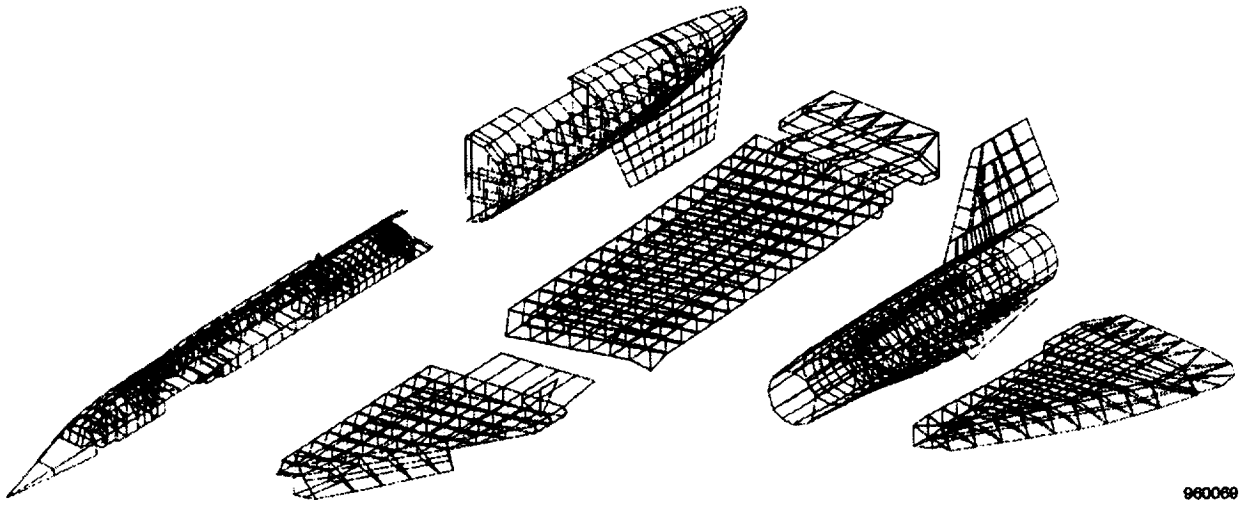

Figure 30. Large NASTRAN structural model of YF-12A airplane (ref. 18).

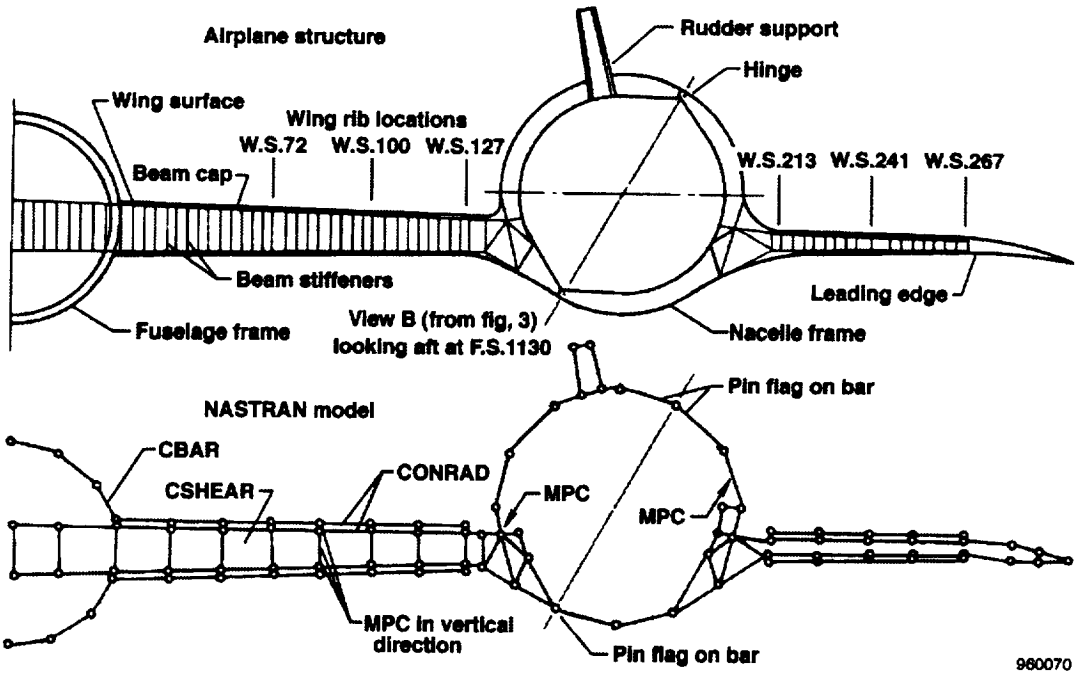

Figure 31. The YF-12A structure and the large NASTRAN model at fuselage station 1130 (ref. 18).

Figure 32 shows a comparison of the predicted shear stresses with those measured for one calibration test condition using the large structural model (fig. 30) (ref.18). Measured shear stresses interpreted from wing strain gages from the load calibration tests are compared to predictions obtained from the large NASTRAN structural model. Some discrepancies were evident between the measured and computed values.

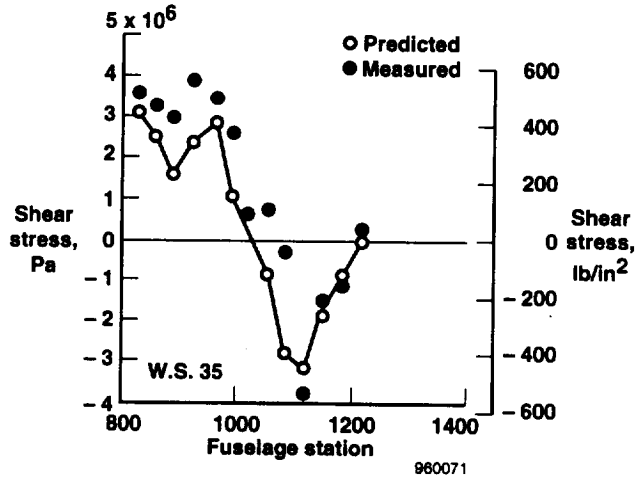

Figure 32. Comparison of NASTRAN-predicted shear stresses with those measured for a calibration test condition (ref. 18).

Figure 33 shows a similar comparison for bending stresses (ref. 18). The measured bending stresses (solid symbols) and the computed bending stresses (open symbols) correlate quite closely.

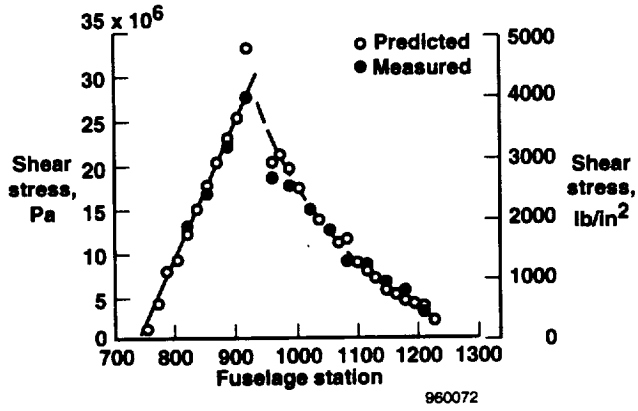

Figure 33. Comparison of NASTRAN-predicted bending stresses with those measured for a calibration test condition (ref. 18).

Comparison of Measured and Computed Deflections

Deflections of the airplane were measured during the load calibration. The predicted deflections derived from the large NASTRAN structural model compared quite closely to the laboratory tests (fig. 34) (ref. 18). These data presented ranges from fuselage centerline deformations (W.S. 0) to deflections near the wing tip (W.S. 290).

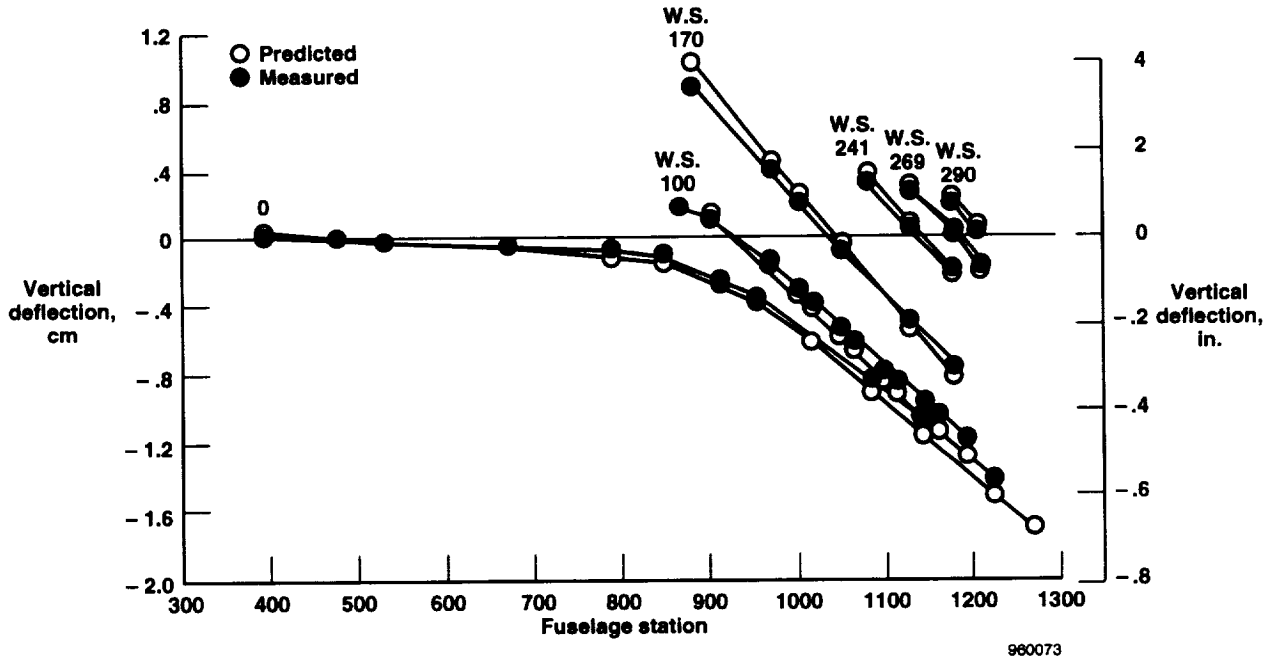

Figure 34. Comparison of NASTRAN-predicted deflections for a typical loading condition (ref. 18).

THERMAL STRESSES AND DEFORMATIONS

Thermal stresses on the YF-12A airplane contributed to much of the difficulty associated with measuring aerodynamic loads with strain gages. The thermal stress measurements were difficult to verify because the strain gages used on the YF-12A airframe were wired as four active arm bridges. These bridges do not lead to the discrete stress measurements required for code verification of thermal stress. Although thermal models were quite detailed, structural models were inadequate in element detail to predict thermal stresses. The thermal deformations of the heated airplane in the laboratory were adequately established and were compared to computed thermal deformations.

Strain Gage Configuration

Four active arm strain gage bridges were used to measure flight loads on the YF-12A airplane (fig. 35). The basic approach is to locate the four arms of the bridge such that all strains are additive, thus maximizing the output. This approach provides summary strains. If the objective is to verify a computational code, then measuring discrete strains is necessary. As a result, a major incompatibility ensues when flight load strain instrumentation is to be used to verify structural models because thermal stress fields are usually quite irregular. The discrete thermal stresses at the location of each of the four active arm strain gages of the bridge is usually of drastically differing magnitudes; therefore, only some average value for the four strain gages is possible.

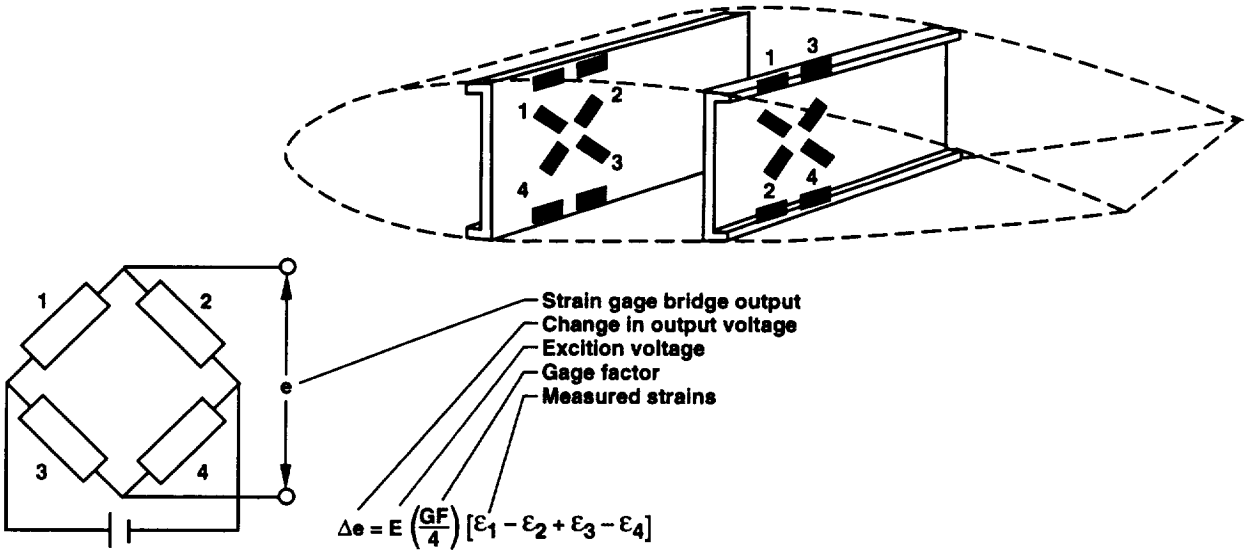

Figure 35. Typical strain gage bridge installation for flight loads measurement.

Prediction of Thermal Stress

The data presented in figures 36(a) and 36(b) illustrate the significance of the thermal component of the total strain gage bridge output. Although the structure was designed to minimize thermal stress, the thermal effects were the significant, and in some cases, the dominant, stress. Note that these data demonstrate that the thermal calibration was necessary to obtain aerodynamic loads.

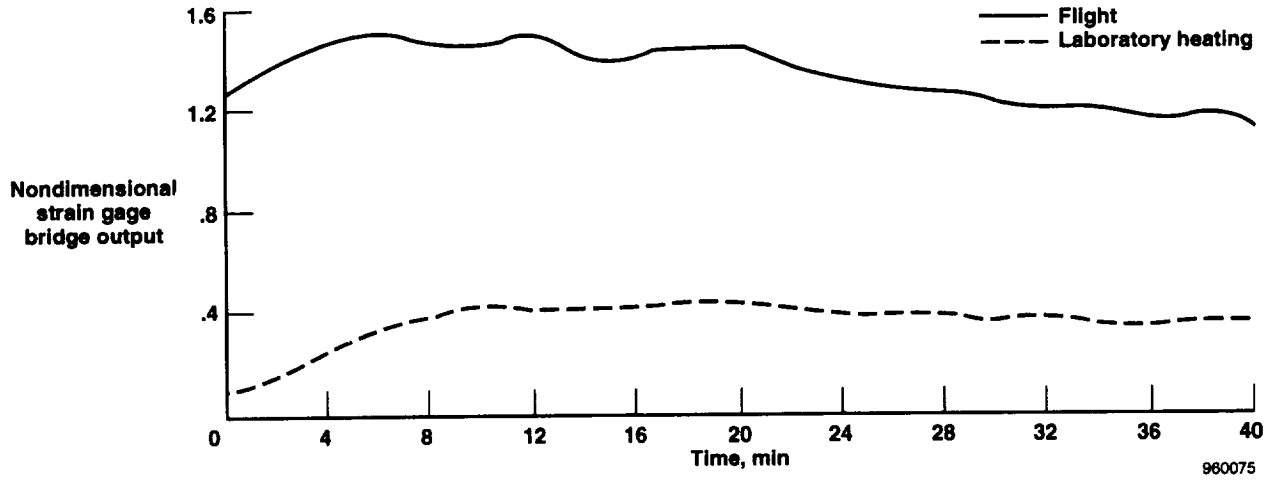

(a) Dominate flight load.

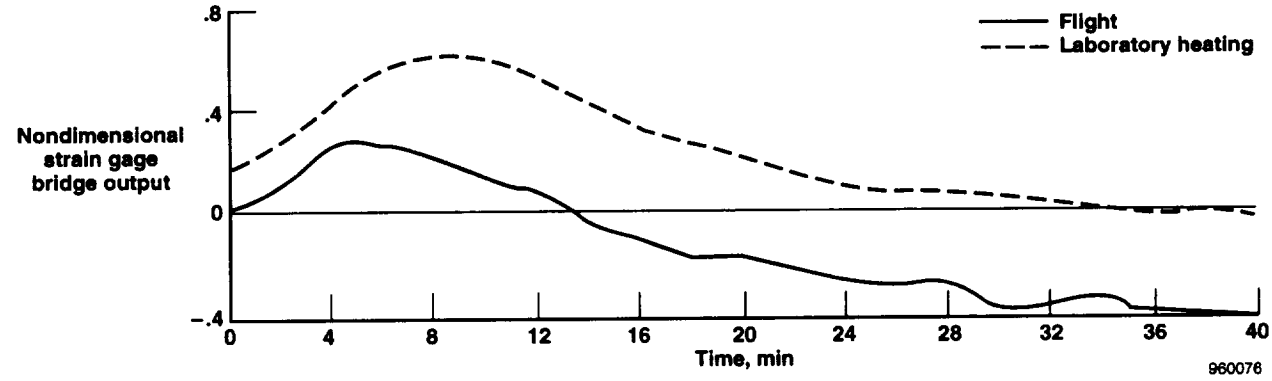

(b) Dominant thermal load.

Figure 36. Comparison of strain gage bridge outputs due to a Mach 3 thermal calibration test and a Mach 3 flight.

Figure 37 shows flight-measured temperatures for four periods (ref. 10). The temperature gradients are greater during the early times of the flight. This density of thermocouple coverage was typical. The number of thermocouples was adequate to ensure that good simulation of the temperature distributions was achieved in the laboratory. On the other hand, the number was inadequate to define the temperature field of the structure for code verification. Verification of structural codes was just too great a task for that era. Considerable structural detail must be incorporated into the modeling to accurately predict temperatures and thermal stresses (refs. 21–23). Attempts to verify thermal stress codes were met with disappointment caused by three factors:

- The structural model detail required was, from a practical point of view, beyond the existing state of the art.
- Strain gage bridges are inappropriate for discrete thermal stress measurement.
- Additional extensive substructure temperature measurements were needed.

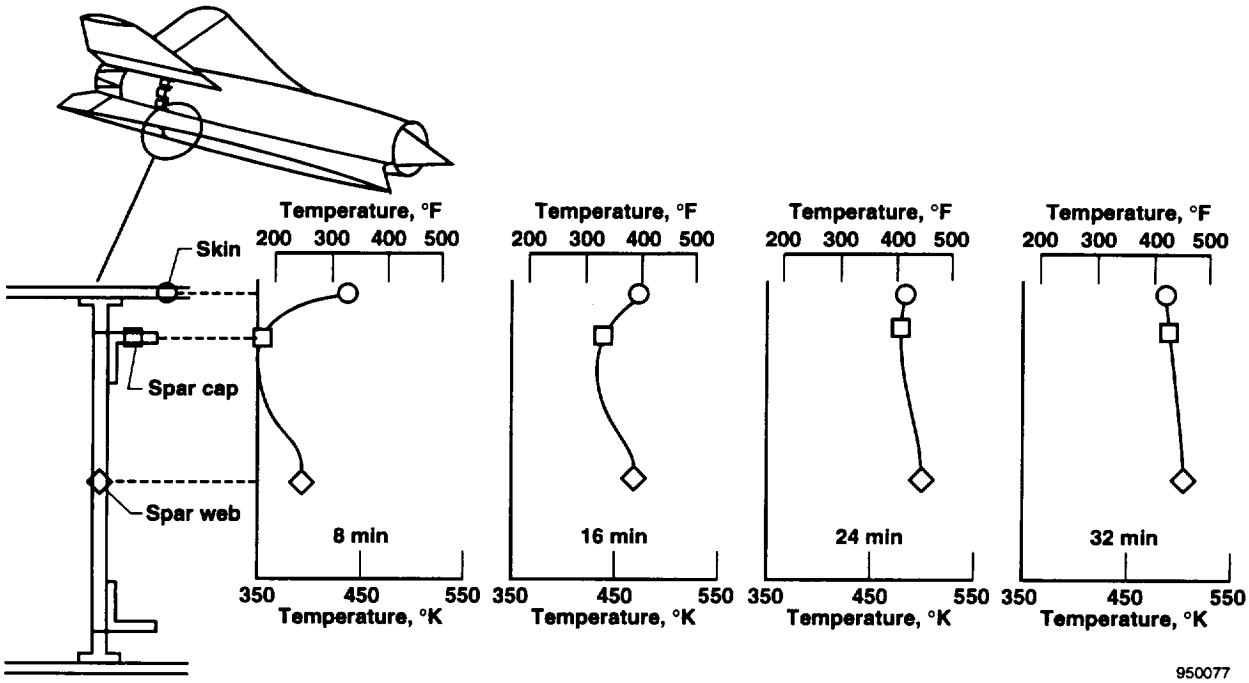

Figure 37. Distribution of typical temperatures in a YF-12A wing spar (ref. 10).

Prediction of Thermal Deformations

Deformations of the airplane were measured in the laboratory during the heating and loading tests and during flight test. Figure 38 shows the camera system used to measure flight deformations (ref. 24). The

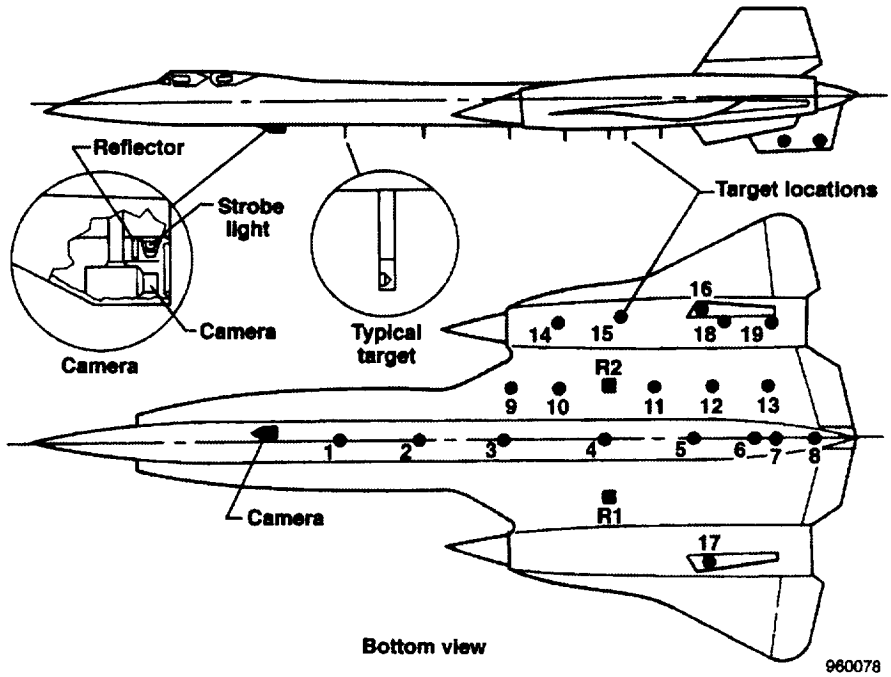

Figure 38. The YF-12A inflight deflection measuring system (ref. 24).

light from a strobe was reflected from corner reflectors mounted on posts which were attached to the airplane. The reflected light was recorded on film photographically, and these data were analyzed using vector graphics. Deflections of the airplane during heating tests were measured with deflection transducers. The large structural model was used to predict the thermal displacements during the heating tests (fig. 30).

Thermal deformations are much easier to predict than discrete stresses. The solid symbols shown in figures 39(a) and 39(b) represent aircraft deformations measured in the laboratory during a heating test (ref. 18). The open symbols represent the deformations predicted with the large NASTRAN structural model for the same heating condition. Correlation between measured and predicted thermal deformation is quite close.

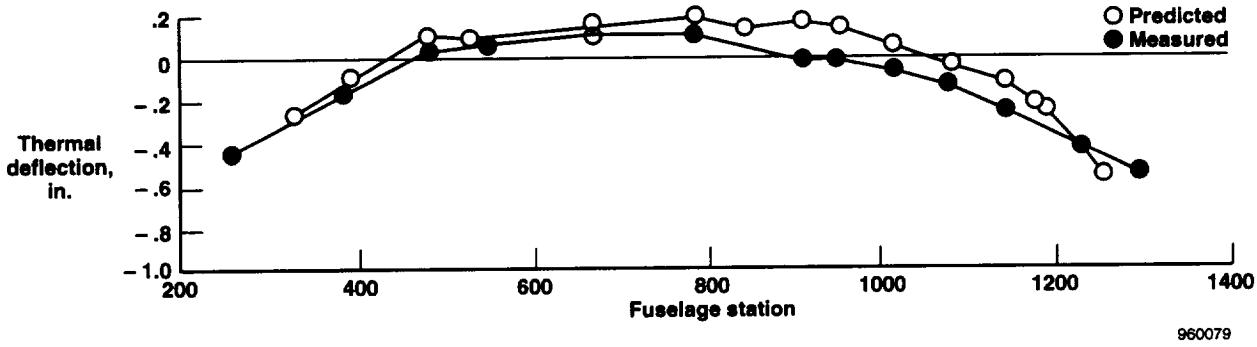

(a) Fuselage centerline.

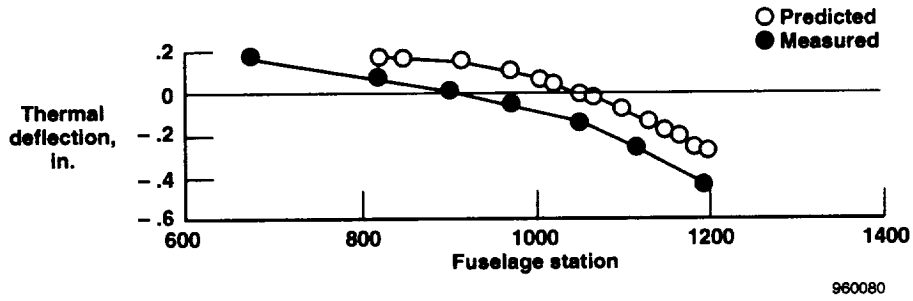

(b) Wing station 35.

Figure 39. Comparison of measured and predicted aircraft thermal deformations for the YF-12A airplane (ref. 18).

CONCLUDING REMARKS

The heating of the YF-12A airplane provided a focus on numerous technological issues that needed defining with regard to aircraft that incorporate hot structures in the design. Laboratory structural heating test technology with infrared systems was predominately created with this program. The program demonstrated the ability to duplicate the complex flight temperatures of an advanced supersonic airplane in a ground-based laboratory. The ability to heat and load an advanced operational aircraft in a laboratory at

high temperatures and to return the aircraft to flight status without adverse effects was also demonstrated. The technology associated with measuring loads with strain gages on a hot structure was demonstrated using the thermal calibration concept.

The results demonstrated that the thermal stresses were significant although the aircraft was designed to reduce thermal stresses. In some cases, the thermal stresses were significantly larger than the load stresses. Very little was learned about how to predict thermal stress although ways to accommodate it in a flight program were learned. The detail required to computer model the heat transfer and the structure became evident. The YF-12A structures and loads effort was a particularly productive effort because a great deal of flight, laboratory test, and computational data were produced and cross-correlated. Much fallout technology was produced, and much insight into the direction of future research was revealed.

Dryden Flight Research Center
National Aeronautics and Space Administration
Edwards, California, October 24, 1995

REFERENCES

1. *NASA YF-12A Flight Loads Program*, NASA TM X-3061, 1974.

2. Banner, Richard D., Albert E. Kuhl, and Robert D. Quinn, *Preliminary Results of Aerodynamic Heating Studies on the X-15 Airplane*, NASA TM X-638, 1962.

3 Quinn, Robert D. and Murray Palitz, *Comparison of Measured and Calculated Turbulent Heat Transfer on the X-15 Airplane at Angles of Attack up to 19.0°*, NASA TM X-1291, 1966.

4. Jenkins, Jerald M., V. Michael DeAngelis, Edward L. Friend, and Richard C. Monaghan, *Flight Measurements of Canard Loads, Canard Buffeting, and Elevon and Wing-Tip Hinge Moments on the XB-70 Aircraft Including Comparisons with Predictions*, NASA TN D-5359, 1969.

5. DeAngelis, V. Michael and Lawrence F. Reardon, *Correlation of Flight-Measured Wing Loads with Wind-Tunnel and Theoretical Predictions for a Variable-Geometry Fighter-Type Airplane*, NASA TM X-1920, 1969.

6. Friend, Edward L. and Richard C. Monaghan, *Flight Measurements of Buffet Characteristics of the F-111A Variable-Sweep Airplane*, NASA TM X-1876, 1969.

7 Fields, Roger, A. and Andrew Vano, *Evaluation of an Infrared Heating Simulation of a Mach 4.63 Flight on an X-15 Horizontal Stabilizer*, NASA TN D-5403, 1969.

8. Quinn, Robert D. and Frank V. Olinger, *Heat-Transfer Measurements Obtained on the X-15 Airplane Including Correlations with Wind-Tunnel Results*, NASA TM X-1705, 1969.

9. Sefic, Walter J. and Karl F. Anderson, *NASA High Temperature Loads Calibration Laboratory*, NASA TM X-1868, 1969.

10. Jenkins, Jerald M. and Albert E. Kuhl, "Summary of Recent Results Pertaining to Strain Gage Load Measurement Technology of High Speed Aircraft," *NASA YF-12 Flight Loads Program*, NASA TM X-3061, 1974, pp. 303–323.

11. Sefic, Walter J. and Lawrence F. Reardon, "Loads Calibration of the Airplane," *NASA YF-12 Flight Loads Program*, NASA TM X-3061, 1974, pp. 61–107.

12. Jenkins, Jerald M., Roger A. Fields, and Walter J. Sefic, *Elevated Temperature Effects on Strain Gages on the YF-12A Wing*, NASA CP-2054, vol. 1, 1978.

13. Quinn, Robert D. and Frank V. Olinger, "Flight Temperatures and Thermal Simulation Requirements," *NASA YF-12 Flight Loads Program*, NASA TM X-3061, 1974, pp. 145–184.

14. Olinger, Frank V., Walter J. Sefic, and Richard J. Rosecrans, "Laboratory Heating Tests of the Airplane," *NASA YF-12 Flight Loads Program*, NASA TM X-3061, 1974, pp. 207–258.

15. Wheaton, Duane L. and Karl F. Anderson, "Laboratory Digital Data Acquisition and Control System for Aircraft Structural Loading and Heating Tests," *NASA YF-12 Flight Loads Program*, NASA TM X-3061, 1974, pp. 185–206.

16. Skopinski, T. H., William S. Aiken, Jr., and Wilber B. Huston, *Calibration of Strain-Gage Installations on Aircraft Structures for the Measurement of Flight Loads*, NACA report 1178, 1954.

17. Jenkins, Jerald M. and Albert E. Kuhl, *A Study of the Effect of Radical Load Distributions on Calibrated Strain Gage Load Equations*, NASA TM 56047, 1977.

18. Curtis, Alan R. and Clay D. Sumpter, "NASTRAN Structured Analysis of the YF-12A Airplane," *NASA YF-12 Flight Loads Program*, NASA TM X-3061, 1974, pp. 435–558.

19. McCormick, Caleb W., ed., The NASTRAN User's Manual (Level 15), NASA SP-222(01), 1972.

20. Jenkins, Jerald M., Albert E. Kuhl, and Alan L. Carter, *The Use of a Simplified Structural Model as an Aid in the Strain Gage Calibration of a Complex Wing*, NASA TM-56046, 1977.

21. Jenkins, Jerald M., *Correlation of Predicted and Measured Thermal Stresses on an Advanced Aircraft Structure with Similar Materials*, NASA TM 72862, 1979.

22. Jenkins, Jerald M., *Comparison of Measured Temperatures, Thermal Stresses, and Creep Residues with Predictions on a Built-Up Titanium Structure*, NASA TM 86814, 1987.

23. Jenkins, Jerald M., "Prediction of Temperature, Thermal Stresses, and Creep in a Loaded and Heated Titanium Structure," *Workshop on Correlation of Hot Structures Test Data with Analysis*, NASA CP-3065, vol. II, 1988.

24. Vano, Andrew and Jon L. Steel, "Measurement of Aircraft Structural Deflections in Flight," *NASA YF-12 Flight Loads Program*, NASA TM X-3061, 1974, pp. 109–144.

REPORT DOCUMENTATION PAGE

Form Approved
OMB No. 0704-0188

Public reporting burden for this collection of information is estimated to average 1 hour per response, including the time for reviewing instructions, searching existing data sources, gathering and maintaining the data needed, and completing and reviewing the collection of information. Send comments regarding this burden estimate or any other aspect of this collection of information, including suggestions for reducing this burden, to Washington Headquarters Services, Directorate for Information Operations and Reports, 1215 Jefferson Davis Highway, Suite 1204, Arlington, VA 22202-4302, and to the Office of Management and Budget, Paperwork Reduction Project (0704-0188), Washington, DC 20503.

1. AGENCY USE ONLY (Leave blank)	2. REPORT DATE	3. REPORT TYPE AND DATES COVERED
	May 1996	Technical Memorandum

4. TITLE AND SUBTITLE

A Historical Perspective of the YF-12A Thermal Loads and Structures Program

5. FUNDING NUMBERS

WU 505-70-63

6. AUTHOR(S)

Jerald M. Jenkins and Robert D. Quinn

7. PERFORMING ORGANIZATION NAME(S) AND ADDRESS(ES)

NASA Dryden Flight Research Center
P.O. Box 273
Edwards, California 93523-0273

8. PERFORMING ORGANIZATION REPORT NUMBER

H-2079

9. SPONSORING/MONOTORING AGENCY NAME(S) AND ADDRESS(ES)

National Aeronautics and Space Administration
Washington, DC 20546-0001

10. SPONSORING/MONITORING AGENCY REPORT NUMBER

NASA TM-104317

11. SUPPLEMENTARY NOTES

12a. DISTRIBUTION/AVAILABILITY STATEMENT

Unclassified—Unlimited
Subject Category 01

12b. DISTRIBUTION CODE

13. ABSTRACT (Maximum 200 words)

Around 1970, the YF-12A loads and structures efforts focused on numerous technological issues that needed defining with regard to aircraft that incorporate hot structures in the design. Laboratory structural heating test technology with infrared systems was largely created during this program. The program demonstrated the ability to duplicate the complex flight temperatures of an advanced supersonic airplane in a ground-based laboratory. The ability to heat and load an advanced operational aircraft in a laboratory at high temperatures and return it to flight status without adverse effects was demonstrated. The technology associated with measuring loads with strain gages on a hot structure was demonstrated with a thermal calibration concept. The results demonstrated that the thermal stresses were significant although the airplane was designed to reduce thermal stresses. Considerable modeling detail was required to predict the heat transfer and the corresponding structural characteristics. The overall YF-12A research effort was particularly productive, and a great deal of flight, laboratory, test and computational data were produced and cross-correlated.

14. SUBJECT TERMS

F-111 aircraft; Flight loads; Heat transfer; Hot structures; Loads measurement; Strain gages; Thermal loads and structures; YF-12A aircraft

15. NUMBER OF PAGES

35

16. PRICE CODE

A03

17. SECURITY CLASSIFICATION OF REPORT	18. SECURITY CLASSIFICATION OF THIS PAGE	19. SECURITY CLASSIFICATION OF ABSTRACT	20. LIMITATION OF ABSTRACT
Unclassified	Unclassified	Unclassified	Unlimited

NSN 7540-01-280-5500

Available from the NASA Center for AeroSpace Information, 800 Elkridge Landing Road, Linthicum Heights, MD 21090; (301)621-0390

Standard Form 298 (Rev. 2-89)
Prescribed by ANSI Std. Z39-18
298-102

National Aeronautics and
Space Administration
Code JTT
Washington, D.C. 20546-0001
USA

Official Business
Penalty for Private Use, $300

SPECIAL FOURTH-CLASS RATE
POSTAGE AND FEES PAID
NASA
PERMIT No G27

POSTMASTER: If Undeliverable (Section 158
Postal manual) Do Not Return